

## Invited paper

Carlos Rodríguez-Navarro\* and Encarnación Ruiz-Agudo

# Nanolimes: from synthesis to application

<https://doi.org/10.1515/pac-2017-0506>

**Abstract:** Cultural heritage objects and structures are subjected to a range of weathering processes that result in their decay and destruction. To slow weathering rates and/or mitigate their effects, several protective and consolidant materials have been used during conservation interventions. Treatments based on organic polymers and alkoxysilanes, as well as some traditional inorganic treatments such as lime water, are in many cases either incompatible and/or show limited efficacy. In recent years nanolimes, that is, dispersions of  $\text{Ca}(\text{OH})_2$  nanoparticles in alcohol (as well as alcohol dispersions of other alkaline-earth metal hydroxide nanoparticles), have emerged as an effective and compatible conservation material. Here we review recent advances in the synthesis and application of nanolimes in the field of heritage conservation. First, we present an overview of lime-based conservation materials, with an emphasis on the earliest reports on the use of nanolimes. Subsequently, we present the different methods used to synthesize nanolimes. Afterwards, we describe their carbonation and its consolidation effects. Practical application of nanolimes in heritage conservation are summarized, including consolidation of stone, ceramics, lime mortars and mural painting, as well as deacidification of paper, canvas, and wood. The advantages and limitations of this novel nanotechnology for cultural heritage conservation are outlined. Finally, some conclusions and areas for future research are presented.

**Keywords:**  $\text{Ca}(\text{OH})_2$ ; carbonation; ChemCultHerit; conservation; consolidation; cultural heritage; deacidification; nanolimes; nanotechnology.


## Introduction

Landmarks of mankind's cultural heritage such as the Sphinx in Egypt, the Buddhist caves along the Silk Road, or the frescoes of the Sistine Chapel, are inexorably decaying and crumbling due to chemical, physical and biological weathering phenomena. These deleterious processes include, but are not limited to, the action of atmospheric pollutants, salt crystallization, hydric and thermal expansion, freeze-thawing, dissolution and hydrolysis, photodegradation, and biodeterioration [1–6]. Their effects can be dramatic: from discoloration and granular disintegration, to scaling, flaking and/or spalling [7], ultimately resulting in the loss of invaluable cultural heritage objects and structures [5]. Several conservation treatments have been developed and applied to mitigate the degradation of heritage materials and to prolong their life expectancy, so that they can safely be part of our cultural legacy to future generations [5]. Traditional treatments for the protection and consolidation of materials, such as stone, mortars and plasters, and mural painting, included synthetic polymers such as acrylic, epoxy or (poly)vinyl resins, as well as their copolymers, and alkoxysilanes [8–10]. Other treatments, both traditional ones such as the barium hydroxide treatment [11], or more recent ones based on (i) the conversion of calcium carbonate into calcium oxalates [12] or (ii) calcium phosphates [13], (iii) the application of calcium alkoxides [14], and (iv) bacterial miner-

**Article note:** A special issue containing invited papers on Chemistry and Cultural Heritage (M.J. Melo, A. Nevin and P. Baglioni, editors).

**\*Corresponding author: Carlos Rodríguez-Navarro**, Department of Mineralogy and Petrology, University of Granada, Fuentenueva s/n, 18002 Granada, Spain, e-mail: carlosrn@ugr.es

**Encarnación Ruiz-Agudo:** Department of Mineralogy and Petrology, University of Granada, Fuentenueva s/n, 18002 Granada, Spain

 © 2017 IUPAC & De Gruyter. This work is licensed under a Creative Commons Attribution-NonCommercial-NoDerivatives 4.0 International License. For more information, please visit: <http://creativecommons.org/licenses/by-nc-nd/4.0/>

Brought to you by | Universidad de Granada

Authenticated

Download Date | 11/22/18 11:36 AM

alization of calcium carbonates [15], have been also applied with varying degree of success. Unfortunately, some of the traditional protective and consolidant materials listed above are in many cases incompatible with the inorganic substrate they are applied to because their composition and physical properties differ. Such an incompatibility may foster damage [16]. Giorgi et al. [17] showed a dramatic example of such an incompatibility. A copolymer treatment (vinyl-acetate/*n*-butyl-acrylate) which was applied on mural paintings affected by salt damage in the Maya site of Mayapan (Yucatan, Mexico) ultimately led to enhanced deterioration (Fig. 1). This was due to the fact that in several cases organic treatments are deposited as a surface film, preventing water vapor transport from the interior of the porous substrate towards the exterior (Fig. 2). If, for instance, salt solutions flowing within the treated porous stone or mortar substrate cannot reach the surface because the treatment film acts as a barrier, they eventually crystallize behind the treatment film as subflorescence, creating crystallization pressure and damage [6], manifested by the detachment of surface scales.

The physicochemical incompatibility and poor aging of most polymer-based conservation treatments [17, 18], in addition to the fact that in many cases their application involved the use of toxic solvents [5], have prompted the resurgence of inorganic conservation materials, which historically were the first used by mankind [19]. This is the case of lime water, a saturated solution of  $\text{Ca}(\text{OH})_2$ , which was traditionally applied to consolidate carbonate-based substrates such as limestone or marble [20]. During carbonation,

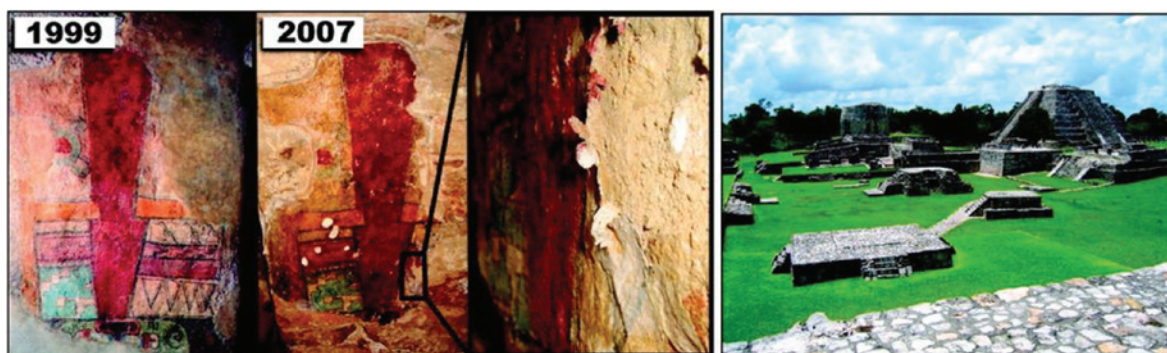


**Fig. 1:** Mural paintings in the “Templo de los Nichos Pintados” at the archeological site of Mayapan (Yucatan, Mexico). The wall painting shows extensive degradation due to flaking associated with salt weathering. This damaging phenomenon is related to the conservation intervention performed in 1999 using a copolymer coating (Mowilith DM5). Reprinted with permission from Giorgi et al. [17]. Copyright 2010 American Chemical Society.

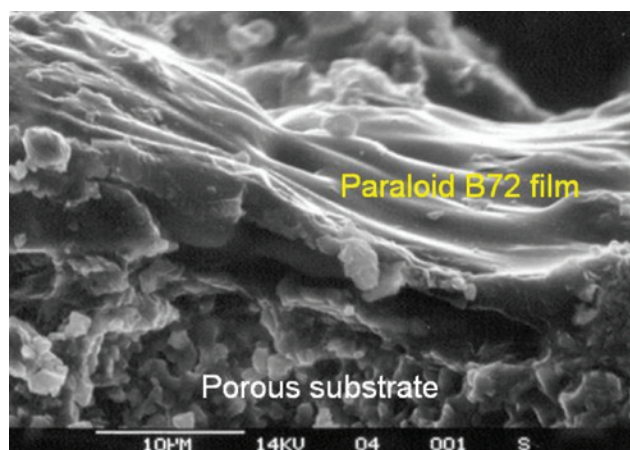


**Fig. 2:** SEM image of a cross-section of calcarenite (limestone) from the Cathedral of Granada treated with an acrylic copolymer (Paraloid B72). The copolymer forms an impervious (detrimental) surface film.

atmospheric CO<sub>2</sub> dissolves in the calcium hydroxide solution, leading to precipitation of calcium carbonate according to the (overall) carbonation reaction:



The newly formed CaCO<sub>3</sub> can act as a cement, binding loose grains and/or filling cracks. However, the lime water method does not seem to be very effective [21]. Apparently, this is principally due to the relatively low solubility of Ca(OH)<sub>2</sub> in water (1.65 g L<sup>-1</sup> at 20 °C) [22], which limits the amount of consolidant that can be introduced into the porous system of the treated material. Such a limitation could be partly overcome by repeated treatment applications: Drdácký et al. [23] reported an acceptable level of consolidation in lime mortars, but only if more than 160 applications of lime water were performed. However, the introduction of large quantities of water within a porous substrate may lead to deleterious side-effects such as substrate dissolution, discoloration, clay-swelling, mobilization of salts (resulting in salt damage), or freeze-thaw damage [19]. Moreover, it has been shown that, in general, the calcium carbonate precipitated out of the lime water applied to porous substrates was a loose powder with little consolidation capacity [24].

To overcome the limitations of the lime water treatment, Giorgi et al. [25] proposed the use of aliphatic alcohol dispersions of portlandite [Ca(OH)<sub>2</sub>] particles synthesized heterogeneously following slaking of quicklime (see following section). The authors reported that aqueous suspensions of portlandite particles were kinetically unstable and settled rapidly. In addition, the higher contact angle and viscosity of water, and the resulting limited sorptivity, prevented the penetration of the particles within the porous substrate, leading to white surface glazing. Basically, when water was used as a dispersion medium, the resulting suspension of portlandite particles was a “white wash” or diluted milk of lime, which has been a traditional and effective surface coating applied on a range of buildings. But its use is not acceptable for stone or mural painting conservation. Remarkably, Giorgi et al. [25] were able to obtain very stable dispersions of Ca(OH)<sub>2</sub> particles using short-chain aliphatic alcohols, a dispersion system that was previously patented by Baglioni et al. [26]. Such a high colloidal stability and the fact that the used aliphatic alcohols have a low surface tension and high sorptivity when applied to porous substrates, enabled an effective consolidation of limestone, lime mortars and mural paintings. A principal advantage of such a treatment was the fact that the solid loading in the alcohol dispersion could be tailored at will (e.g. up to 50 g/L), so that an amount substantially higher than that introduced using lime water could be applied to a porous substrate. Moreover, the rapid evaporation of the alcohol ensured that within hours the substrate would be solvent-free. Because an alcohol was used as dispersing solvent, none of the drawbacks associated with the application of water were detected. Remarkably, the carbonation of portlandite nanoparticles has been shown to produce a coherent CaCO<sub>3</sub> cement able to bind the mineral grains in the treated substrate, leading to its strengthening and effective consolidation [27]. Overall, the new method overcame the main limitations of the lime water treatment, and had none of the drawbacks of organic polymer and alkoxysilane treatments applied on carbonate substrates, other than the use of volatile organic compounds (VOCs), i.e. short-chain aliphatic alcohols, as dispersing media (see below the discussion on potential health effects of nanolimes).

Nonetheless, slaked lime is known to be highly polydisperse [28] as shown in Fig. 3. Hence, in Giorgi and co-workers' [25] pioneering study, both nanometer-sized primary particles as well as micrometer-sized particles and aggregates were present. Although this study set the path for the development of nanolimes as novel effective conservation nanomaterials, the alcohol dispersions used could not strictly be considered as nanolimes. In subsequent studies Baglioni's group succeeded in the homogeneous synthesis, characterization and application in cultural heritage conservation of alcoholic dispersions of Ca(OH)<sub>2</sub> nanoparticles with size typically below 500 nm, which can be considered as true nanolimes. In 2002 the authors filled two patents where the methodology for the synthesis and application of nanolimes was outlined [29, 30]. From that point on, significant progress has taken place in the synthesis, characterization and application of nanolimes as a multipurpose conservation nanomaterial that is reviewed in the following sections.

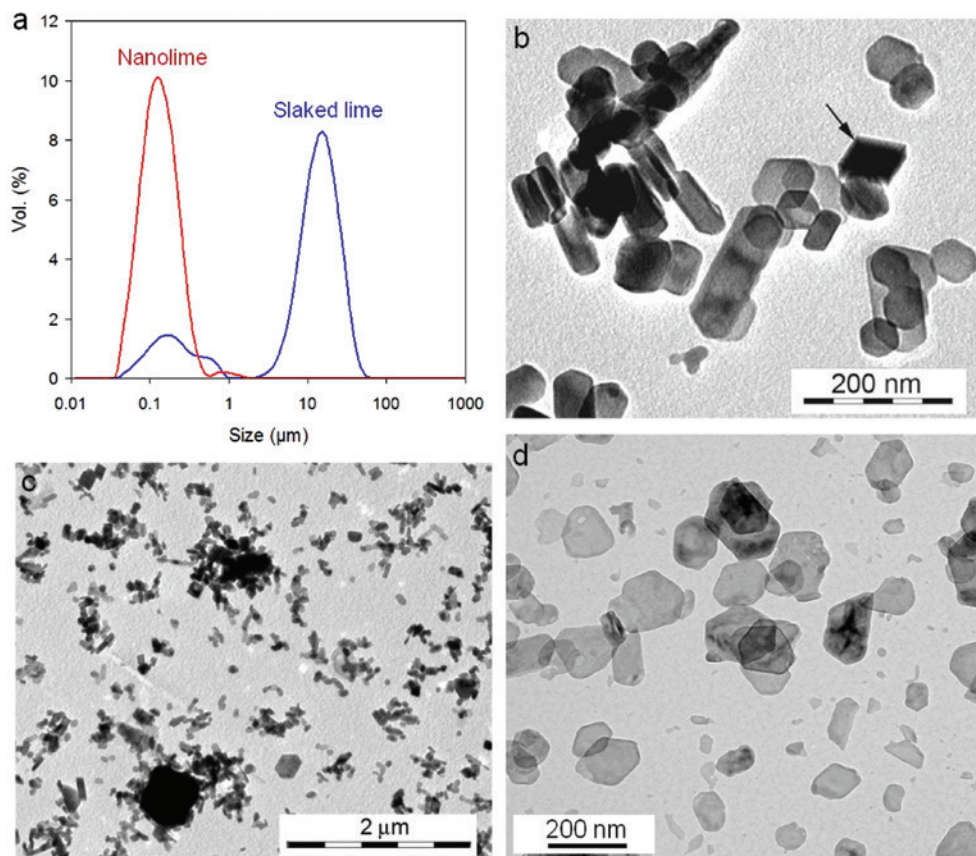


**Fig. 3:** Particle size distribution (PSD) and nanostructural features of slaked limes and nanolimes: (a) PSD of a typical slaked lime and a commercial nanolime (CaLoSiL<sup>®</sup>); TEM photomicrographs of (b) primary hexagonal plate-like nanoparticles (the arrow points to a calcite rhombohedron) and (c) larger aggregates in slaked lime putty, and (d) well-dispersed nanoparticles in a commercial nanolime (CaLoSiL<sup>®</sup>). Parts (b) and (c) reproduced with permission from Rodríguez-Navarro et al. [27]. Copyright 2013 American Chemical Society.

## Synthesis of nanolimes

Two basic routes have been explored for the synthesis of nanolimes: heterogeneous and homogeneous synthesis [17, 28, 31–34]. The first includes the traditional procedure for the preparation of  $\text{Ca}(\text{OH})_2$ , i.e. lime slaking, as well as novel routes based on precursor alkoxides and metallic calcium, while the second (with many variants) involves the precipitation of nanolimes in an aqueous (or hydroalcoholic) solution via chemical reaction of dissolved species. Below we present an overview of both routes.

### Heterogeneous synthesis

#### Lime slaking

Lime ( $\text{CaO}$ ) is a vernacular material used for building and decorative purposes for millennia [35]. First evidences for the use of slaked lime as a binder in mortars and plasters date back to ca. 12 000–14 000 years before present, corresponding to the advent of pyrotechnology in the Near East [36]. The traditional technology for the production of slaked or hydrated lime, which was subsequently used for multiple applications (not only for building or decorative purposes, but also for a range of technical applications such as food processing, disinfection, or leather tanning, just to name a few examples), involved a series of heterogeneous

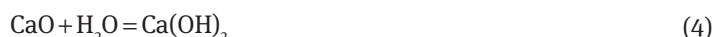
reactions, which along with carbonation, constitute the so-called “lime cycle” [22, 35]. First, carbonate stones (e.g. limestones) are calcined at temperatures above 850–900 °C via the following solid-state (topotactic) reaction [37]:



If dolostones are used instead of limestones, the following overall solid-state reaction (also topotactic) takes place [38]:



The resulting lime, or the mixture of lime and periclase (MgO), is subjected to hydration. This is a highly exothermic process known as lime slaking which results in the formation of portlandite via the reaction [39, 40]



in the case of calcitic limes, while it also involves the hydration of periclase forming brucite ( $\text{Mg}(\text{OH})_2$ ), via the reaction



when dolomitic limes are used. For the sake of simplicity, hereafter we will only refer to the heterogeneous synthesis of  $\text{Ca}(\text{OH})_2$ , that is high-calcium limes.

Traditional lime slaking typically involved the mixing of quicklime with an amount of water higher than the stoichiometric amount, thereby resulting in an aqueous dispersion of  $\text{Ca}(\text{OH})_2$  particles. Such a dispersion is known as lime putty and has been the preferred binder for the preparation of lime-based mortars and plaster since ancient times [35]. If the stoichiometric amount of water (or a slight excess) is added to the oxide, dry hydrated lime is produced, which is the standard modern industrial product of lime hydration [22]. In both cases, as stated above, the hydration of calcium oxide results in portlandite particles with a highly heterogeneous size distribution [28]. Hydration of lime typically results in two classes of particles ranging from the nano- to the micrometer size: hexagonal plate-like primary nanoparticles with size ranging from a few tenths to a few hundred nanometers, and larger aggregates of the former particles (up to several micrometers) [28] (Fig. 3b and c). Such a heterogeneity in the particle size distribution as well as the existence of large aggregates, some of them formed via oriented attachment and therefore very hard to redisperse because of their irreversible aggregation [28], might be favorable for the consolidation of highly porous substrates with large pores [33, 41]. It is, however, a strong handicap for most applications as alcohol dispersions (i.e. as nanolimes). Indeed, a prerequisite for the successful application of nanolimes for the consolidation of artworks is that their size has to be sub-micrometric, ideally <300 nm [17, 33, 42], so that they are able to penetrate deeply into the pore system of the treated materials. Moreover, a high surface area and reactivity (e.g. towards carbonation) is critical, which is not only associated with their nanosize, but also with their crystal shape, a plate-like habit being optimal [43].

Although it is known that the conversion of calcium oxide into portlandite crystals of various size and habit is affected by many factors, including the reactivity of the oxide and the retention of heat through control of the water to oxide ratio [22, 35], unfortunately, traditional lime slaking offers limited control on these two key features of  $\text{Ca}(\text{OH})_2$  particles. There are, however, different alternatives to reduce the size and degree of aggregation of slaked lime and to control its crystal shape. One is the aging of slaked lime putty [44]. This is a traditional procedure used since Roman times to improve the quality of lime putties [45]. It involves the long term storage (months to years) of slaked lime putty pastes under water (or more precisely, lime water). Aging results in a reduction in particle size (and a parallel increase in surface area) via the formation of sub-micrometer sized plate-like portlandite crystals [44]. Such aged lime putties display faster carbonation, and a high water retention, workability and improved rheology (higher dynamic viscosity) [39, 43, 46]. Alcohol dispersions prepared using such aged lime putties have been shown to be highly stable, being effective consolidants when applied to porous stones such as sandstone [27].

Another route to achieve  $\text{Ca}(\text{OH})_2$  nanoparticles via heterogeneous synthesis is related to the production of acetylene gas following hydration of calcium carbide via the (overall) reaction



The resulting “carbide lime” is an impure lime putty, which typically is land-filled or discarded in open ponds as a waste material. However, the particle shape and size (sub-micrometer plate-like  $\text{Ca}(\text{OH})_2$  particles) and high surface area ( $>30 \text{ m}^2/\text{g}$ ) of carbide lime make it a very good candidate for the preparation of nanolimes following its dispersion in short-chain alcohols. By using a patented purification process [47], Rodríguez-Navarro et al. [27] were able to prepare ethanol and propan-2-ol carbide lime dispersions which were successfully applied as “nanolimes” for the consolidation of porous stone.

Slaked limes with a high surface area and large amounts of plate-like  $\text{Ca}(\text{OH})_2$  nanoparticles can also be obtained by using additives such as lignosulfonates dosed in the slaking water. Such additives were applied in the past as a means to improve the reactivity of heterogeneously precipitated  $\text{Ca}(\text{OH})_2$  particles used for the capture of combustion flue-gases (e.g.  $\text{SO}_2$ ) [48, 49]. Similarly, by using hydroalcoholic mixtures (methanol, ethanol, propan-1-ol or di-ethylene glycol) during lime slaking, the formation of abundant  $\text{Ca}(\text{OH})_2$  nanoparticles with very high surface area ( $>45 \text{ m}^2/\text{g}$ ) has been achieved [50, 51]. However, this route has not yet been exploited for the preparation of nanolimes used in the conservation of cultural heritage.

In addition to the previous bottom-up approaches for the formation of nanosized  $\text{Ca}(\text{OH})_2$  crystals during lime slaking, there are alternative top-down approaches. These involve the reduction in crystal (or aggregate) size of portlandite particles present in slaked or hydrated lime via high- $T$  milling [52], mechanical homogenization [53], and/or ultrasonication [54]. Such top-down methods have been successfully used for the preparation of nanolimes with multiple applications in heritage conservation.

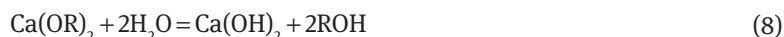
Despite the above mentioned limitations of lime slaking for producing monodisperse sub-micrometer portlandite particles, it should be pointed out that the high yield and reduced cost of this route have not been surpassed by any of the synthesis routes that are described below.

### Sol-gel and solvothermal synthesis

An effective route for the heterogeneous synthesis of nearly monodisperse  $\text{Ca}(\text{OH})_2$  nanoparticles was patented by Ziegenbalg [55]. In this case, the preparation of aliphatic alcohol nanolime dispersions involved the use of a sol-gel/solvothermal method. Basically it consisted in the initial synthesis of precursor calcium alkoxides (methoxides, ethoxides, propoxides or isopropoxides), which is easily achieved by reacting metallic Ca with the corresponding alcohol at a relatively high  $T$  ( $>60 \text{ }^\circ\text{C}$ ) according to the well-known reaction [56, 57]



where M is an alkaline-earth metal, typically Ca, Mg, Sr or Ba, and R typically is a methyl, ethyl or  $n$ -propyl group. Note, however, that the release of  $\text{H}_2$  gas during reaction (7) can pose a risk. Ziegenbalg [55] proposed the direct application of alkaline-earth alkoxide solutions (the solvent being an alcohol) for the consolidation of carbonate substrates. A very similar approach was followed by Favaro et al. [14]. Ziegenbalg [55] suggested the application of  $\text{H}_2\text{O}$  or to take advantage of the humidity present in the substrate/environment to achieve the formation of calcium hydroxide in situ, within the porous substrate, via the hydrolysis reaction,



Such an hydrolysis reaction could be induced prior to treatment application, leading to the formation of nanometric  $\text{Ca}(\text{OH})_2$  particles that could subsequently be applied as an alcohol dispersion. Carbonation of the resulting  $\text{Ca}(\text{OH})_2$  would lead to the consolidation of the treated substrate. In 2006, nanolimes synthesized using an alkoxide route were given the trade name CaLoSil<sup>®</sup>, and after extensive testing they have been commercialized since 2010 by IBZ-Salzchemie GmbH & Co. KG (Germany). This product has found widespread application in cultural heritage conservation [23, 58–60].

One principal advantage of this synthesis route is that it yields alcohol nanolime dispersions without additives (e.g. surfactants, see below) or reaction by-products that might require further purification steps (as occurs in several homogeneous synthesis processes, see below). Moreover, the formation of  $\text{Ca}(\text{OH})_2$  crystals during reaction (8) typically occurs in an homogeneous fashion within the bulk hydroalcoholic solution, at a very high supersaturation. This leads to a high nucleation density and limited coarsening due to classical crystal growth (including Ostwald ripening, that is, the growth of the larger particles at the expenses of the smallest) or non-classical coarsening via nanoparticle aggregation [61]. Apparently, aggregation is limited by chemi- and/or physi-sorption of the alcohol present in the synthesis solution onto  $\text{Ca}(\text{OH})_2$  nanoparticles [62]. Moreover, the adsorbed short-chain aliphatic alcohol enables a high colloidal stabilization of the nanoparticles dispersed in such a continuum phase. This occurs via hydrophobic interactions [63]. As shown in Fig. 3a and d, the resulting nanolimes are nearly monodisperse and, typically, the  $\text{Ca}(\text{OH})_2$  crystals are thin hexagonal plates with size  $\sim 30\text{--}300$  nm.

It is relevant to note that such a route for the production of nanosized oxides and hydroxides was already explored back in the 1990s. Indeed, precipitation of sparingly soluble alkaline-earth hydroxides was achieved based on the sol–gel technique [64]. For instance,  $\text{Ca}(\text{OH})_2$  nanoparticles were synthesized by Koper et al. [65] using such a route. First, Ca-methoxide was prepared at room  $T$  by reacting metallic Ca with methanol. The resulting methoxide was dissolved in methanol-toluene and subjected to hydrolysis at room  $T$ . Following sol–gel transition, the gel was transferred to an autoclave and treated at high  $T$  ( $265^\circ\text{C}$ ) and  $P$  (41 atm). The system was subsequently vented and cooled to room  $T$ . Nanosized  $\text{Ca}(\text{OH})_2$  crystals were thus obtained. A similar route was previously used for the synthesis of  $\text{Mg}(\text{OH})_2$  nanoparticles [66]. In these studies, however, the ultimate goal was to achieve nanosized alkaline-earth metal oxides following thermal decomposition of the precursor hydroxides. No potential applications of the resulting hydroxides in heritage conservation were considered. Remarkably, the sol–gel route above described was not foreign to the conservation community at the time. The Battelle method for paper deacidification, which was presented in 1994, involved the use of alkaline-earth alkoxides and the products of their (easy) hydrolysis (e.g. Mg hydroxide) and carbonation (hydrous magnesium carbonates) [67].

Poggi et al. [68] used a variation of the solvothermal alkoxide route for the synthesis of nanometric  $\text{Ca}(\text{OH})_2$  crystals that were dispersed in ethanol or propan-1-ol and applied for conservation purposes. Synthesis was achieved at high  $P$  and  $T$  in an autoclave. In a first step, calcium alkoxides were synthesized at  $70^\circ\text{C}$  or  $130^\circ\text{C}$  by reacting metal Ca granules with ethanol or propan-1-ol, respectively. In a second step, the synthesized alkoxides were subjected to hydrolysis in an hydroalcoholic solution at  $70^\circ\text{C}$  to obtain colloidal  $\text{Ca}(\text{OH})_2$ , which was in turn dispersed in ethanol or propan-1-ol prior to application. The choice of alcohol used during synthesis had a clear effect on the particle size distribution. Ethanol synthesis led to  $\text{Ca}(\text{OH})_2$  particles with a bimodal size distribution, with relative maxima at 80 and 220 nm. Conversely, synthesis in propan-1-ol led to an unimodal particle size distribution centered at 260 nm. The resulting nanolimes were successfully applied for deacidification of cellulose-based artifacts [68] and water-logged wood pieces [69].

Borsoi et al. [41] implemented another solvothermal route for the synthesis of nanolimes which was based on the hydration of metallic calcium. Granulated metallic Ca was reacted in water under  $\text{N}_2$  atmosphere at a relatively high  $T$  ( $90^\circ\text{C}$ ). Portlandite formed via the following heterogeneous reaction,



Upon elimination of the supernatant solution and dispersion in alcohol or, in some cases, water (or hydroalcoholic solutions), nanolimes ready for application were obtained. Typically, the resulting precipitate was made up of  $\text{Ca}(\text{OH})_2$  nanoparticles with size ranging from 50 to 600 nm, which over time (96 h) tended to develop micrometer-sized aggregates. This synthesis route does not seem to achieve the small particle size of the previous solvothermal method (alkoxide precursor). Nonetheless, the resulting nanolimes have found successful application in artwork conservation.

An innovative route for the formation of nanosized  $\text{Ca}(\text{OH})_2$  particles was proposed by Liu et al. [70]. Nanoparticles formed via a hydrogen plasma-metal reaction (HPMR). The authors used metallic Ca ingots covered with an oxidized layer (i.e. CaO) that were subjected to arc-melting in an Ar- $\text{H}_2$  atmosphere.  $\text{Ca}(\text{OH})_2$

nanoparticles with average size of 100 nm (based on TEM observations) and 28.7 m<sup>2</sup>/g surface area were achieved via vapor deposition. The authors reported that the yield rate (0.5 g/min) was higher than that of homogeneous synthesis routes, and concluded that such nanoparticles could be applied for cultural heritage conservation.

## Homogeneous synthesis

Despite the fact that abundant Ca(OH)<sub>2</sub> nanoparticles with a high surface area can be achieved using high-yield heterogeneous synthesis routes such as the classic lime slaking process, it has proved very difficult to achieve monodispersity or to control the particle size and shape via the latter synthesis route. This is why Ambrosi et al. [71, 72] proposed an homogeneous synthesis route for the production of Ca(OH)<sub>2</sub> nanoparticles with a tight particle size distribution that could be used as nanolimes for conservation purposes.

### Aqueous precipitation routes

Previous studies on the homogeneous synthesis of a range of metal hydroxide nanoparticles, including Ca(OH)<sub>2</sub>, showed that by properly selecting/controlling reaction parameters such as *T* and reactant concentration, which in turn determine the system supersaturation, nearly monodisperse nanosized precipitates could be achieved [62, 73]. Based on such a knowledge, Ambrosi et al. [71] mixed previously heated (60–90 °C) concentrated (up to 0.4 M) CaCl<sub>2</sub> and (up to 0.8 M) NaOH (or KOH) solutions under nitrogen atmosphere (to avoid carbonation) and vigorous stirring. Precipitated Ca(OH)<sub>2</sub> was separated from the supernatant and the NaCl byproduct was eliminated by repeated washing with water. The resulting hexagonal plate-like portlandite nanoparticles, with hexagonal sides <300 nm in size (i.e. with overall particle size <600 nm, measured along the diagonal of the hexagon), were dispersed in different aliphatic alcohols and the nanolime dispersions were fully characterized. They were shown to be very stable if compared with water-portlandite dispersions. Their application on different substrates such as stone, bricks, tiles and lime mortars [72], wood [74], paper and canvas [53], and mural painting [33, 71] demonstrated that such homogeneously-synthesized nanolimes were highly efficient consolidants or deacidification agents. This synthesis route was patented by Baglioni's group [29, 30] and the nanolime alcohol dispersions prepared by such a route have been commercially available since 2008 under the trade-name Nanorestore®. Subsequent studies by Baglioni's group and others improved this synthesis route by selecting the optimal reaction *T* (90 °C), adding NaOH drop-wise to a CaCl<sub>2</sub> solution [75], eliminating NaCl via dialysis [76] or, to avoid the dissolution of the most reactive Ca(OH)<sub>2</sub> nanocrystals (i.e. those of the smallest size and therefore more soluble according to the Gibbs-Thomson effect [61]), using lime water instead of deionized water during NaCl elimination [33, 74].

Several variations to this synthesis route have been proposed. The effect of changing the Ca source was explored by Samanta et al. [77] who used a Ca(NO<sub>3</sub>)<sub>2</sub> solution to which NaOH was added drop-wise (at 30 °C). The resulting nanoparticles were very similar to those previously obtained by Baglioni's group. Daniele and Taglieri [78] used Triton X-100 (a non-ionic surfactant) to favor the formation of nanosized Ca(OH)<sub>2</sub> crystals following mixing of CaCl<sub>2</sub> and NaOH concentrated solutions. The authors reported that the surfactant prevented the aggregation of primary Ca(OH)<sub>2</sub> nanoparticles and led to more reactive nanolimes that carbonated at a very high rate. Moreover, the presence of the surfactant speeded up the synthesis process, as there was no need to add NaOH drop-wise as in previous methods in order to achieve plate-like nanoparticles with hexagonal side dimensions 50–400 nm. Nonetheless, repeated washing with water was required to eliminate reaction byproducts and the surfactant. As an ecological alternative to the use of surfactants, Darroudi et al. [79] used a gelatin solution dosed with calcium chloride to which NaOH solution was added drop-wise (at 90 °C). The milky precipitate was centrifuged and washed several times with distilled water to eliminate residual NaCl and organics. The authors reported that this nanolime had an average particle size of 600–650 nm.



Despite the use of a “green” organic, the relatively large  $\text{Ca}(\text{OH})_2$  crystal size does not seem to offer any significant advantage compared to previous art. Other organic additives were previously used for the synthesis of nanosized  $\text{Ca}(\text{OH})_2$ . Xu et al. [80] used poly-vinyl acrylate or poly-ethylene glycol to produce  $\text{Ca}(\text{OH})_2$  particles 50–100 nm in size, following mixing of  $\text{CaCl}_2$  and NaOH solutions (NaOH was dosed drop-wise) under sonication. Despite the thorough washing of the particles (to eliminate reaction byproducts), thermogravimetric analysis showed that a significant amount of polymer was still present. It is not known if the presence of such polymers may affect the performance of the nanoparticles when used as nanolimes in conservation interventions.

### Synthesis in diols

Based on previous work on the synthesis of nanosized metal hydroxides ( $\text{In}(\text{OH})_3$ ) in ethylene glycol at a relatively high  $T$ , which were dispersed by peptization with propan-1-ol [81], Salvadori and Dei [82] proposed an alternative route for the homogeneous synthesis of nanophase  $\text{Ca}(\text{OH})_2$ . It involved the hydrolysis of  $\text{CaCl}_2$  solutions in 1,2-ethanediol (or 1,2-propanediol) via drop-wise addition of an aqueous solution of NaOH at 150 °C. However, it was necessary to eliminate the adsorbed diol. This was achieved by peptization in propan-2-ol under sonication. Extensive testing demonstrated that the resulting nanolimes were effective consolidants for limestone, tiles and lime-based wall paintings [83], most likely due to the fact that the  $\text{Ca}(\text{OH})_2$  particles had a size of 30–60 nm and, once peptized, formed stable alcohol dispersions. A variation to this route was proposed by Roy and Bhattacharya [84] who dissolved calcium nitrate in ethane-1,2-diol (ethylene glycol) at 115 °C. To this solution, NaOH was added drop-wise under vigorous stirring. To remove ethylene glycol, the dispersion was peptized using propan-2-ol and the solids were separated by centrifugation (the process was repeated five times). The resulting  $\text{Ca}(\text{OH})_2$  nanoparticles had an average size of 35 nm. Note, however, that Giorgi et al. [17] have pointed out that the use of ethylene glycol appears to be detrimental, because it fosters aggregation of the nanoparticles [63], and it is difficult to eliminate. Moreover, Chelazzi et al. [33] indicate that this route is time-consuming and produces a scarce amount of nanoparticles.

### Use of W/O microemulsions

Pioneering works on the use of microemulsions for the synthesis of  $\text{Ca}(\text{OH})_2$  nanoparticles was reported in 1990s. Delfort et al. [85] used a synthesis route that involved the hydrolysis of calcium hydride in the presence of a surfactant in an emulsion made with mineral oil, methanol-toluene, water, and tetrahydrofuran. After precipitation of nanosized  $\text{Ca}(\text{OH})_2$ , volatile solvents were eliminated via vacuum evaporation and mineral oil was eliminated by dialysis in *n*-heptane. The authors proposed that  $\text{Ca}(\text{OH})_2$  precipitation occurred at the same time as micellation in a water-in-oil (W/O) microemulsion. The  $\text{Ca}(\text{OH})_2$  crystals were plate-like and 12–30 nm in size. The problem with this synthesis route is its complexity and the need for several purification steps. In any case, this route produced  $\text{Ca}(\text{OH})_2$  nanoparticles a few nanometer in size, which, as pointed out by Nanni and Dei [86], could not be achieved by any of the common routes used for the preparation of nanolimes. To achieve such a small size, Nanni and Dei [86] also used W/O microemulsions. This route takes advantage of the ability of microdroplets to compartmentalize reactants in discrete aqueous nanodomains [64]. Microdroplets were obtained with the help of a nonionic surfactant. Such microdroplets were loaded with  $\text{Ca}^{2+}$  and  $\text{OH}^-$  in separate microemulsions. Upon mixing of the microemulsions and after prolonged reaction time (up to 48 h)  $\text{Ca}(\text{OH})_2$  nanoparticles with an average size of 5 nm were obtained. Despite the potential of such extremely small nanoparticles for the preparation of very reactive nanolimes, Chelazzi et al. [33] pointed out that the low production yield and the complex and time consuming synthesis procedure make the application of these particles in conservation interventions almost unfeasible.

### Ion-exchange resins

Recently, Taglieri et al. [87] proposed the use of an anion-exchange resin (Dowex Monosphere 550A (OH)) for the production of nanolimes. Granules of such a resin were pre-loaded with  $\text{OH}^-$  in a NaOH solution. Subsequently, the resin granules were dispersed in a concentrated  $\text{CaCl}_2$  solution. Following the exchange of  $\text{OH}^-$  by  $\text{Cl}^-$  in the resin, a high supersaturation was reached (homogeneously) within the bulk aqueous solution, leading to the precipitation of nanosized  $\text{Ca}(\text{OH})_2$  crystals at room  $T$ . Separation of the resin granules and supernatant solution led to pure  $\text{Ca}(\text{OH})_2$  particles that were subsequently dispersed in an alcohol. The main advantage of this synthesis route is the fact that no purification process (e.g. washing) was required after precipitation, as no dissolved by-products (e.g. chloride ions) were left in solution. Moreover, the exhausted resin can be regenerated for further synthesis of nanolime. More recently, the authors demonstrated that this route for nanolime production was cost-effective and could be scaled up [88].

### Insolubilization-precipitation

Bastone et al. [89] proposed a route for the homogeneous synthesis of nanolime using an insolubilization-precipitation method. It consisted in the addition of an alcohol (propan-2-ol) to lime water. Upon mixing, a nanosized  $\text{Ca}(\text{OH})_2$  precipitate was obtained. This was previously observed by one of our PhD students, Kudlacz [90], who mixed lime water and ethanol in a 1:2 v/v ratio. This researcher reported that right after mixing, the solution became milky-like. TEM observations revealed that this was due to the precipitation of nearly monodisperse portlandite nanoparticles  $\sim 150\text{--}300$  nm in size (Fig. 4). According to Kudlacz [90], addition of ethanol into lime water caused a sudden increase in the supersaturation with respect to portlandite, which promoted the formation of abundant  $\text{Ca}(\text{OH})_2$  nuclei and limited their growth. The author indicated that this was due to the fact that ethanol strongly reduces the water activity. Bastone et al. [89] observed that an increase in the reaction  $T$  from 40 up to 76 °C led to a reduction in particle size (down to 7–37 nm). Remarkably, some of the particles did not display the standard hexagonal-plate morphology of portlandite,

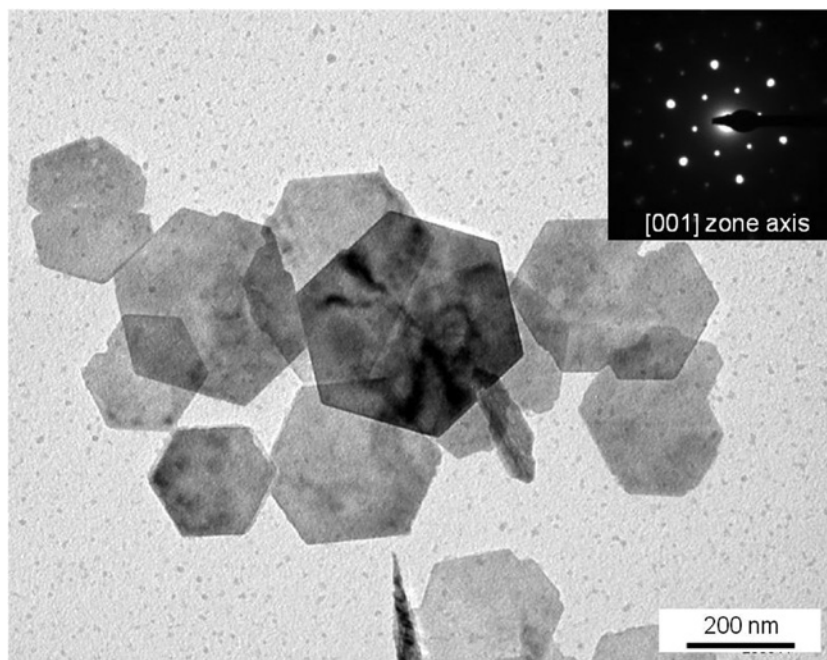


**Fig. 4:** Hexagonal plate-like nanoparticles synthesized via mixing of lime water and ethanol at room  $T$  [90]. The inset shows the  $[001]_{\text{portlandite}}$  zone-axis SAED pattern of one of the plate-like crystals. Image courtesy of K. Kudlacz.

but a spherical shape. It was not clear, however, if such spherical particles were indeed portlandite or a calcium isopropoxide or even an amorphous calcium hydroxide phase. Although not explicitly stated by Bastone et al. [89], the alcohol was not only instrumental in inducing a high supersaturation via reduction of the water activity; its adsorption onto newly formed  $\text{Ca}(\text{OH})_2$  nuclei could also limit their growth (i.e. the adsorbed alcohol likely acted as a capping agent [62]). All in all, such a method led to nanosized  $\text{Ca}(\text{OH})_2$  dispersions that were very effective for paper deacidification. It should be noted, however, that per each liter of starting lime water a maximum of  $\sim 1.65$  g of  $\text{Ca}(\text{OH})_2$  can be precipitated after alcohol addition. This seems to be a handicap for the large-scale production of nanolimes using this route.

## Synthesis of other (non-Ca) alkaline-earth nanodispersions

In addition to  $\text{Ca}(\text{OH})_2$ , other alkaline-earth metal hydroxides have been synthesized for their application as nanodispersions. These include  $\text{Mg}(\text{OH})_2$ ,  $\text{Ba}(\text{OH})_2$  and  $\text{Sr}(\text{OH})_2$  nanoparticles that have been applied on a range of cultural heritage materials following their dispersion in short-chain alcohols.

Early works on the synthesis of  $\text{Mg}(\text{OH})_2$  explored both heterogeneous and homogeneous routes [33]. For instance, as indicated above, the heterogeneous synthesis of  $\text{Mg}(\text{OH})_2$  nanoparticles via a sol–gel route was first reported by Utamapanya et al. [66]. Ding et al. [91] obtained monodisperse brucite crystals with an average size of 50 nm via an homogeneous phase synthesis route involving the direct mixing of dilute aqueous solutions of  $\text{Mg}(\text{NO}_3)_2$  and NaOH, followed by hydrothermal aging for 2 h at 80 °C. With a focus on the application of  $\text{Mg}(\text{OH})_2$  as nanolimes for paper conservation, Giorgi et al. [92] studied the effect of different Mg salts on the particle size of  $\text{Mg}(\text{OH})_2$  synthesized via homogeneous precipitation. They mixed different Mg salts solutions with NaOH at 90 °C. The resulting precipitate was then washed to eliminate the byproducts of the reaction (sodium salts). Finally, the nanoparticles were dispersed in alcohol prior to application on paper. Interestingly, the authors observed that the particle size strongly depended on the type of counterion and followed the Hofmeister series. The smallest (and therefore more reactive) nanoparticles ( $\sim 50$  nm) were obtained using magnesium sulfate. Dispersion in alcohol of such nanoparticles outperformed standard methods for paper deacidification.

Considering the long tradition regarding the use of  $\text{Ba}(\text{OH})_2$  solutions for the consolidation of carbonate substrates [11], especially those affected by calcium sulfate damage (e.g. wall painting affected by gypsum crystallization) [19], the synthesis of nanosized  $\text{Ba}(\text{OH})_2$  which could be used in the conservation of cultural heritage was explored [52]. However, this is challenging due to the fact that the high supersaturation required for the homogeneous synthesis of nanoparticles is difficult to achieve in the case of  $\text{Ba}(\text{OH})_2$  because this phase is moderately soluble ( $K_{\text{sp}} = 2.55 \times 10^{-4}$  at 25 °C) [33]. A top-down approach involving milling (at high  $T$  and  $P$ ) of  $\text{Ba}(\text{OH})_2$  crystals dispersed in short-chain alcohols was adopted to achieve nanoparticles with size as small as 100 nm [32]. Nonetheless, it seems that the typical size of the particles obtained via this top-down approach ranges from 200 to 400 nm [33, 52]. Interestingly, unlike  $\text{Ca}(\text{OH})_2$  nanoparticles which form stable dispersions in ethanol, propan-2-ol and propan-1-ol, stable dispersions of  $\text{Ba}(\text{OH})_2$  nanoparticles were only obtained using propan-1-ol. A principal advantage of the use of  $\text{Ba}(\text{OH})_2$  nanoparticles dispersed in short-chain alcohols is the fact that they are not toxic [32]. In contrast, aqueous solutions of barium hydroxide, such as those used in the Ferroni-Dini method for consolidation of wall painting, are highly toxic [32, 52].

$\text{Sr}(\text{OH})_2$  nanoparticles were synthesized homogeneously by Ciliberto et al. [93]. The authors used the same protocol developed for the synthesis of  $\text{Ca}(\text{OH})_2$  nanolimes discussed above. Basically, to a 0.7 M  $\text{Sr}(\text{NO}_3)_2$  solution, a 0.3 M NaOH solution was added drop-wise at 60 °C. Once precipitation was complete, the dispersion was aged for 1 h under intense stirring. Subsequently, the supernatant was eliminated and the solids were washed repeatedly to eliminate residual sodium nitrate. Finally, the aqueous dispersion was sonicated for 30 min. Remarkably, the  $\text{Sr}(\text{OH})_2$  nanoparticles were nearly monodisperse with an average size of 20–40 nm. This is quite an achievement considering that  $\text{Sr}(\text{OH})_2$  is moderately soluble ( $K_{\text{sp}} = 3.2 \times 10^{-4}$  at 25 °C). These nanoparticles could be a viable alternative to toxic  $\text{Ba}(\text{OH})_2$  aqueous solutions for the conversion

of  $\text{CaSO}_4 \cdot 2\text{H}_2\text{O}$  damaging wall paintings into an insoluble sulfate (celestite,  $\text{SrSO}_4$ ), and may help protect limestone or marble by forming a  $\text{SrCO}_3$  surface layer, less soluble than the calcite in the substrate.

## Carbonation of nanolimes

Once nanolimes are applied to a porous substrate and the alcohol has evaporated, carbonation starts following reaction with atmospheric  $\text{CO}_2$ . Carbonation is the main mechanism responsible for the consolidation effect of  $\text{Ca}(\text{OH})_2$  nanoparticles [25, 94–96]. The resulting  $\text{CaCO}_3$  crystals also play a buffer role in deacidification treatments of wood and paper [34]. In this section we will discuss the carbonation of nanolimes considering  $\text{Ca}(\text{OH})_2$  nanoparticles. It should be noted, however, that although the end-products are different, there are several commonalities between the carbonation of  $\text{Ca}(\text{OH})_2$  and other alkaline-earth metal hydroxides such as  $\text{Mg}(\text{OH})_2$ ,  $\text{Ba}(\text{OH})_2$  and  $\text{Sr}(\text{OH})_2$ .

### The carbonation reaction

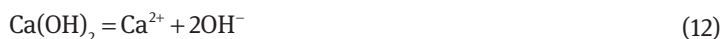
The overall carbonation reaction in eq. (1) shows that one mole of  $\text{Ca}(\text{OH})_2$  will react with one mole of atmospheric  $\text{CO}_2$  to produce one mole of  $\text{CaCO}_3$  plus one mole of  $\text{H}_2\text{O}$ . The newly formed calcium carbonate (i.e. calcite), which has a molar volume 12.6 % higher than portlandite, will more effectively fill the pore space occupied by the precursor nanolime particles, and will consolidate the porous structure by binding mineral grains, as shown in Fig. 5. Despite its apparent simplicity, the carbonation of portlandite is, however, a complex process. First, under standard application conditions (room  $T$  and atmospheric  $p\text{CO}_2$  of  $\sim 10^{-3.5}$  atm), the carbonation of nanolime does not take place according to reaction (1). Such a reaction can only take place at a high  $T$  via a solid state mechanism [97], which seems to be catalyzed by product  $\text{H}_2\text{O}$  [98, 99]. At room  $T$ , carbonation only takes place in the presence of water, via a dissolution-precipitation process [95]. Indeed, extensive research has shown that in the absence of water, no carbonation of  $\text{Ca}(\text{OH})_2$  crystals takes place in air at low  $T$  [95, 98–100]. Only when the relative humidity (RH) is sufficiently high ( $\text{RH} \gg 30\%$ ) significant carbonation is detected [100]. The presence of water, either in bulk or as an adsorbed film is thus critical to enable the dissolution of both  $\text{Ca}(\text{OH})_2$  and atmospheric  $\text{CO}_2$  for the carbonation reaction to take place according to the following series of reactions [60, 95, 101]. Atmospheric  $\text{CO}_2$  dissolves in water and undergoes hydrolysis,



and, subsequently, bicarbonate ions dissociate into carbonate ions



The last reaction is strongly pH-dependent and is favored at high pH. A high pH is achieved by the dissolution of portlandite in pore and/or adsorbed water



which also leads to an increase in the calcium activity of the aqueous solution in contact with portlandite crystals. Ultimately, carbonation takes place in the aqueous phase via the reaction



Reaction (10) is considered the rate controlling step in the overall carbonation process. Note, however, that under the high pH conditions ( $\text{pH} = 12.4$ ) resulting from the dissolution of portlandite, the hydration of  $\text{CO}_2$  can take place at a significantly higher rate via the reaction [102]

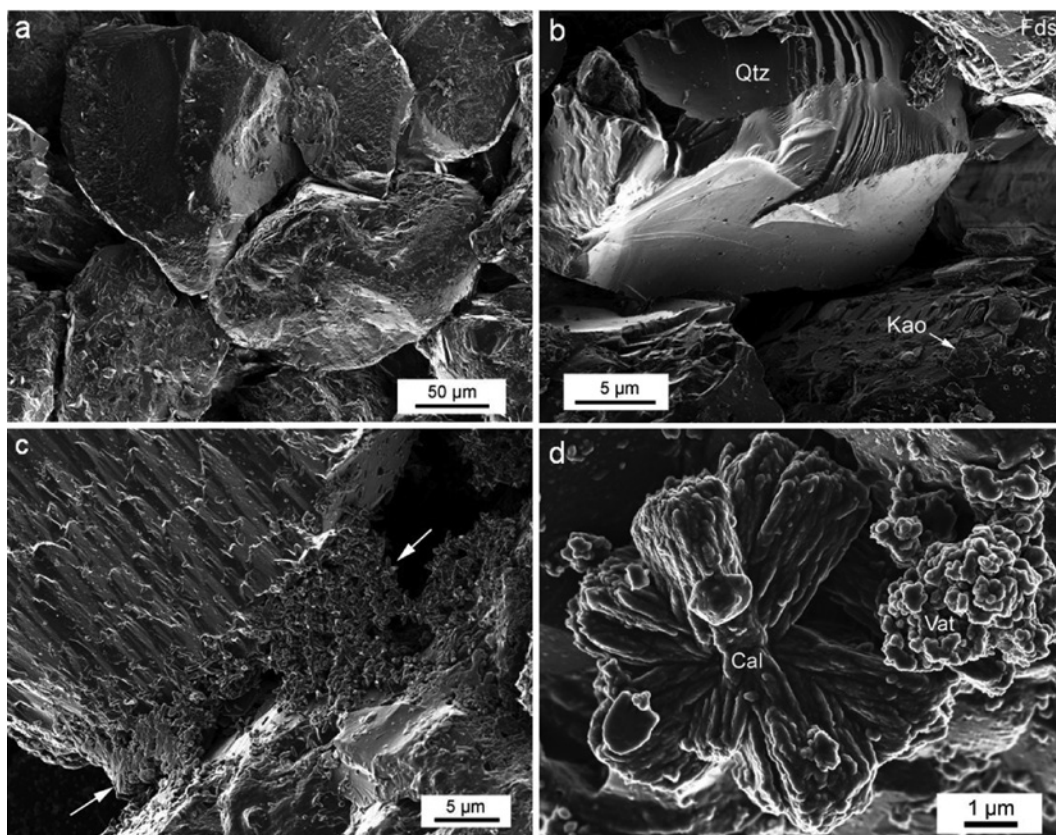


**Fig. 5:** Cementation of quartz grains in a porous sandstone following application of nanolimes: SEM photomicrographs of the sandstone prior (a, and detail in b) and after treatment (c, and detail of newly formed carbonates in d). The arrows in (c) show the location of the  $\text{CaCO}_3$  cement (formed after carbonation of  $\text{Ca(OH)}_2$  nanoparticles) binding two stone grains. Qtz, quartz; Kao, kaolinite; Fds, feldspar; Cal, calcite; Vat, vaterite. Figure parts (b) and (c), reproduced with permission from Rodriguez-Navarro et al. [27]. Copyright 2013 American Chemical Society.



followed by the rapid dissociation of bicarbonate ions into carbonate ions according to reaction (11).

The kinetics of carbonation not only depend on the hydration of  $\text{CO}_2$ , but also on other parameters such as reactant surface area, RH,  $T$ , and  $p\text{CO}_2$ , in addition to impurities/additives (e.g. Mg ions and organic additives) [95, 98, 100, 103]. These parameters, and the RH in particular, can strongly affect the system supersaturation, which ultimately controls the nucleation density of carbonate phases and their evolution [95].

## The role of relative humidity

The carbonation rate of  $\text{Ca(OH)}_2$  nanoparticles and final yield (i.e. fractional conversion of  $\text{Ca(OH)}_2$  into  $\text{CaCO}_3$ ), as well as the resulting  $\text{CaCO}_3$  phase(s) can vary significantly depending on the relative humidity [27, 32], and so does the effectiveness of nanolime treatments [27].

Several studies have underlined the crucial role of humidity in determining the rates of carbonation of portlandite crystals in air at low  $T$  [98, 100, 104]. Shih et al. [98] observed negligible carbonation at  $\text{RH} < 8\%$ , whereas rates exponentially increased with increasing RH. AFM observations by Yang et al. [105] showed that only at  $\text{RH} \geq 30\%$   $\text{CaCO}_3$  precipitated on the surface of portlandite crystals. The latter results are consistent with those of Beruto and Botter [100] who concluded that the formation of an adsorbed (liquid-like) water film on  $\text{Ca(OH)}_2$  particles was critical for carbonation to progress. These authors observed a significant increase in carbonation rate at  $\text{RH} > 70\%$ , when multilayer water adsorption took place. Dheilly et al. [106] pointed

out that at  $RH \gg 30\%$ ,  $\text{CO}_2$  and  $\text{Ca}(\text{OH})_2$  could dissolve in the adsorbed water film present on portlandite so as to enable the precipitation of  $\text{CaCO}_3 \cdot \text{H}_2\text{O}$  released after the carbonation of portlandite could subsequently catalyze the carbonation reaction until completion, or until a passivating  $\text{CaCO}_3$  layer prevented further carbonation [107].

Numerous studies have confirmed that indeed RH is a critical parameter in the carbonation of nanolimes. Faster and more thorough (higher yield) carbonation was systematically observed with increasing RH from 33% up to 95% [75, 104, 108–110]. The humidity conditions not only affected the carbonation rate and yield, but also affected the calcium carbonate polymorph selection and ratio (see below). Ultimately, it was acknowledged that a more effective consolidation following application of nanolimes on porous substrates was achieved when carbonation took place at a relatively high RH (>70%).

Note that typically, a 100% conversion of nanolime into calcium carbonate is difficult to achieve. To overcome this limitation, and considering the impact of humidity on nanolime carbonation, Daniele and Taglieri [111] investigated the effect that the addition of water (in different amounts) had on the carbonation rate and yield of nanolime dispersions. They observed that pure propan-2-ol nanolime dispersions typically resulted in a limited carbonation yield (a few percent under their low 40% RH conditions). Conversely, they observed that the yield could be dramatically increased by preparing water/alcohol binary mixtures. A 1:1 water/propan-2-ol mixture resulted in the highest carbonation yield (70%). It follows that the presence of a fractional amount of water in the alcohol dispersion of nanolime would be advisable for practical conservation applications.

To increase the carbonation yield, Daniele et al. [75] proposed the addition of a carbonate source. They achieved this goal by adding baking soda. However, the authors did not consider the possibility of a reaction between  $\text{Na}_2\text{CO}_3$  and  $\text{Ca}(\text{OH})_2$  resulting in  $\text{CaCO}_3$  plus NaOH. The last product can readily carbonate in the presence of atmospheric  $\text{CO}_2$  and humidity, resulting in deleterious precipitation of sodium carbonate salt crystals (e.g. trona and natron). More recently, López-Arce et al. [112] proposed an alternative method to increase the carbonation rate and yield of nanolimes based on yeast fermentation. Under a high RH, yeast fermentation, which was achieved by mixing yeast and sugar in an aqueous solution, resulted in a concentration of up to 5000 ppm  $\text{CO}_2$  within 2 h, leading to a 100% carbonation after 28 days. They applied this modified nanolime treatment to porous limestones and observed an improvement in the mechanical properties, more significant than in the case of limestone specimens treated with pure nanolime.

In any case, a ~100% carbonation yield can be achieved (in air at relatively high RH) in a reasonable time (weeks to months) only if the  $\text{Ca}(\text{OH})_2$  crystals making up the nanolime have a thickness measured along [001] below a threshold limit. For thicker particles, the formation of a sufficiently thick passivating layer of product  $\text{CaCO}_3$  will hamper further progress of the carbonation reaction towards the core of portlandite particles [95, 107]. Ruiz-Agudo et al. [107] showed that during the initial stages of carbonation in humid air, a porous calcium carbonate surface layer forms that enables the progress of the reaction towards the core of portlandite particles. However, this product layer rapidly becomes impervious due to further  $\text{CaCO}_3$  growth, thereby acting as a passivating layer. Ruiz-Agudo et al. [107] also showed that large portlandite crystals (mm-sized) typically develop cracks along basal planes during carbonation due to stress associated with the molar volume differences between reactant and product phases. However, such cracks that could expose fresh  $\text{Ca}(\text{OH})_2$  for the carbonation reaction to progress, had a very limited effect: only a small volume fraction of such crystals (1.5%) was carbonated after 20 days exposure to humid air [107]. Nanolime dispersions made up of hexagonal plate-like crystals with thickness measured along [001]  $\geq 30$  nm (typical value for coarse slaked lime putty particles) [28, 39], have been shown to never reach a carbonate yield higher than 40% when dispersed in alcohol (as nanolimes) and subjected to carbonation in air at 80% RH and 20 °C for more than 2 months [27, 113]. Conversely, nanolimes with hexagonal plate-like  $\text{Ca}(\text{OH})_2$  crystals with average thickness ~25 nm, reached a nearly 100% carbonation in just 4 days under the same experimental conditions [95]. These results suggest that the key parameter for a high carbonation yield may not be the size (or equivalent diameter) of the nanolime particles, which is measured along [100] or [110], but their actual thickness. In other words,

synthesis processes that can prevent  $\text{Ca}(\text{OH})_2$  nanoparticle growth along [001] might result in nanolimes with best performance towards carbonation. One way to limit growth normal to the basal face is the addition of alcohols during synthesis [62].

## Calcium carbonate phase evolution

The carbonation of nanolimes does not readily results in the formation of the most stable calcium carbonate phase under STP conditions, which is calcite. Numerous studies have shown that different metastable calcium carbonate phases can precede the formation of stable calcite during the carbonation of nanolimes. López-Arce et al. [104, 108] and Gomez-Villalba [109, 110] showed that depending on the RH conditions, metastable calcium carbonate phases such as amorphous calcium carbonate (ACC; with a general formula  $\text{CaCO}_3 \cdot n\text{H}_2\text{O}$ ), monohydrocalcite ( $\text{CaCO}_3 \cdot \text{H}_2\text{O}$ ), and the anhydrous polymorphs vaterite and aragonite, typically formed in different amounts prior to or along with calcite.

Rodriguez-Navarro et al. [95] showed that, in fact, ACC was the dominant phase during the early stages of nanolime carbonation in air at room  $T$ . This metastable phase accounted for up to 24 wt% of the carbonate phases formed during the first 24 h of carbonation at a high RH ( $80 \pm 5\%$ ). Remarkably, this phase formed pseudomorphically after portlandite via a tightly interface-coupled dissolution-precipitation process. Also, ACC precipitated homogeneously in the solution resulting from the dissolution of portlandite. Subsequently, dissolution of ACC led to the formation of vaterite and aragonite, following the mechanism recently revealed by Nielsen et al. [114] using in situ fluid-cell TEM. The growth of vaterite structures after ACC took place via a non-classical nanoparticle-mediated process, where primary vaterite nanoparticles formed through heterogeneous nucleation onto ACC, and aggregated by mesoscale assembly into (nearly)iso-oriented structures (that resembled mesocrystals) [95]. A similar process was suggested for the case of aragonite spindle-like aggregates [95]. Finally, both abundant vaterite, which represented up to 35 wt% of the newly formed carbonates, and minor aragonite (up to 5 wt%) underwent dissolution, which was followed by calcite precipitation. Overall, the carbonation process followed the Ostwald's step rule, represented by the sequence: ACC  $\rightarrow$  vaterite  $\rightarrow$  aragonite  $\rightarrow$  calcite. It should be noted that the full consolidation capacity of nanolimes is not achieved until stable calcite is formed, a process that can take several months. Indeed, it has been experimentally demonstrated that the presence of vaterite following carbonation of nanolimes results in a poorer consolidation of porous stone (sandstone) than that achieved following calcite precipitation [27]. However, we will show below that the conversion of metastable polymorphs (vaterite and aragonite) into stable calcite, can take place in just a few months.

From the previous results, a crucial question emerges: What is the cause (or causes) that promotes the precipitation of metastable phases? In the case of ACC, the high supersaturation reached during carbonation of nanolimes fully explains its initial formation [115]. However, it is not clear why abundant vaterite (and minor aragonite) forms. Several studies have demonstrated that the presence of short-chain alcohols in the reaction medium favors the nucleation and kinetic stabilization of vaterite and aragonite (at room  $T$ ) [116]. It is also known that  $\text{Ca}(\text{OH})_2$  nanoparticles dispersed in ethanol and propan-2-ol react with the solvent forming a surface layer of calcium alkoxides, which can not be removed by desorption (evaporation) of the alcohol at STP conditions [27, 113]. Such a calcium alkoxide surface layer can be (partially) hydrolyzed following water adsorption onto portlandite during carbonation. This way, an hydroalcoholic solution will be present during portlandite carbonation, thereby inducing the formation of vaterite (and aragonite) [95]. Remarkably, Rodriguez-Navarro et al. [95] showed that a heat treatment ( $100^\circ\text{C}$  for 1 h) of the same nanolime producing vaterite (and aragonite), led to the precipitation of pure calcite after ACC following carbonation in air at 80 % RH. The heat treatment resulted in the nearly complete elimination of adsorbed alkoxide/alcohol. As a result, the amount of alcohol present during carbonation was negligible. These results, which are summarized in the scheme of Fig. 6, demonstrate the critical role that alcohol plays in the formation and (partial) stabilization of metastable calcium carbonate polymorphs and their  $t$ -evolution.

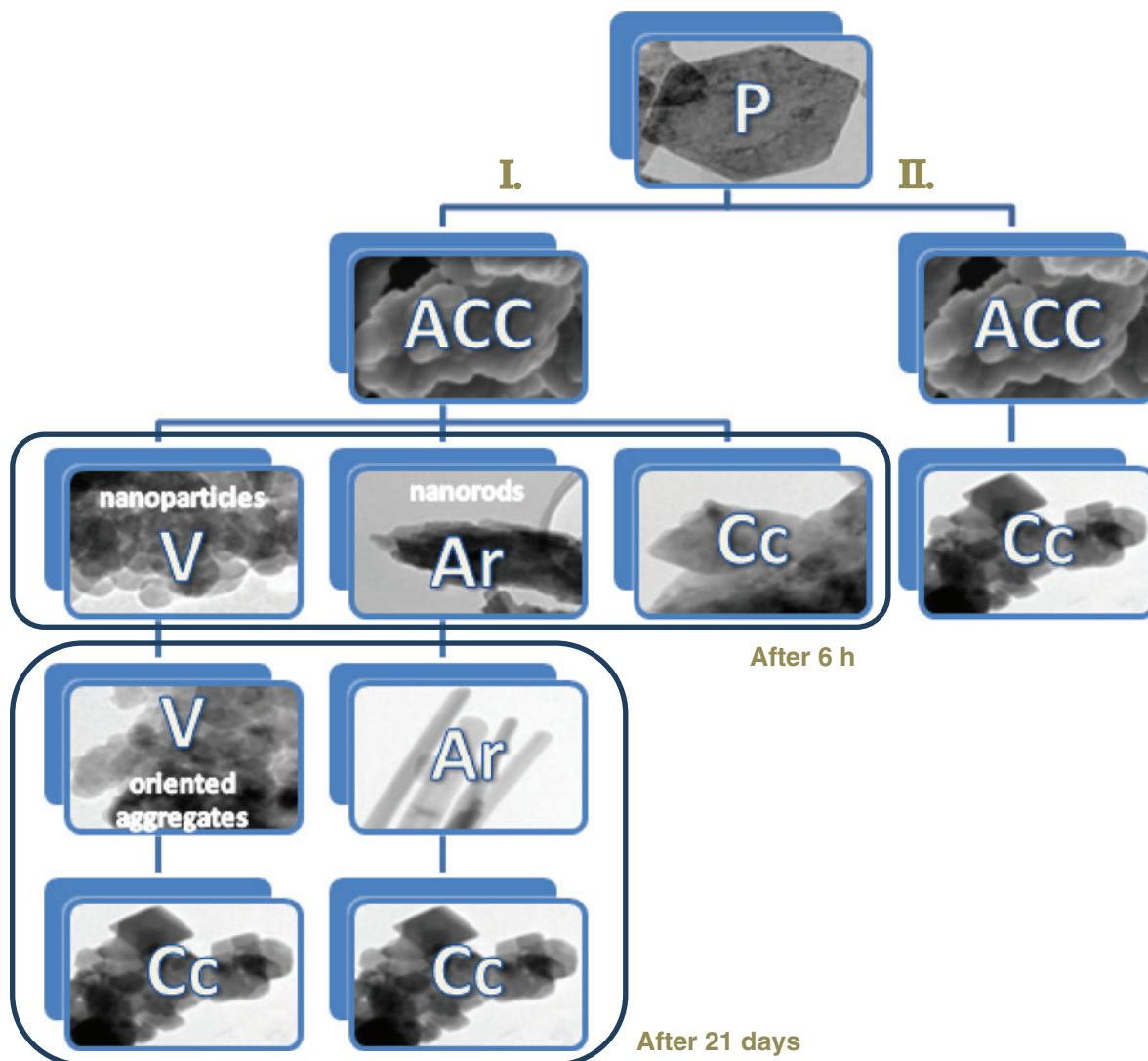


**Fig. 6:** Crystallization paths of nanolime during carbonation in air in the presence and absence of adsorbed alcohol/alkoxide. The scheme shows the phase, mesostructure and morphology of precipitates (TEM images) and their temporal evolution in the presence (route I.) and absence (route II.) of adsorbed ethanol/ethoxide. P, portlandite; ACC, amorphous calcium carbonate; V, vaterite; Ar, aragonite; Cc, calcite. Reproduced from Rodriguez-Navarro et al. [95] with permission from The Royal Society of Chemistry.

## Carbonation kinetics

The speed of carbonation (i.e. the carbonation rate) is of paramount importance if a fast and effective consolidation of the damaged substrate is the target of a nanolime treatment. In other words, nanolime carbonation kinetics are crucial during conservation interventions. Quantitative analyses of the carbonation kinetics have been performed. Carretti et al. [117] and Baglioni et al. [42] showed that the  $t$ -evolution of nanolimes carbonation could be fitted to an Avrami-Erofeev equation,

$$\alpha = 1 - \exp(-kT^n) \quad (15)$$

where  $\alpha$  is the fractional conversion of  $\text{Ca}(\text{OH})_2$  into  $\text{CaCO}_3$ ,  $k$  is the reaction rate constant, and  $n$  is the reaction exponent or order (related to the nucleation type: i.e. dimensionality of the product phase, type of growth, and nucleation rate). A very good fit to this kinetic model was observed for  $\alpha$  values determined from FTIR



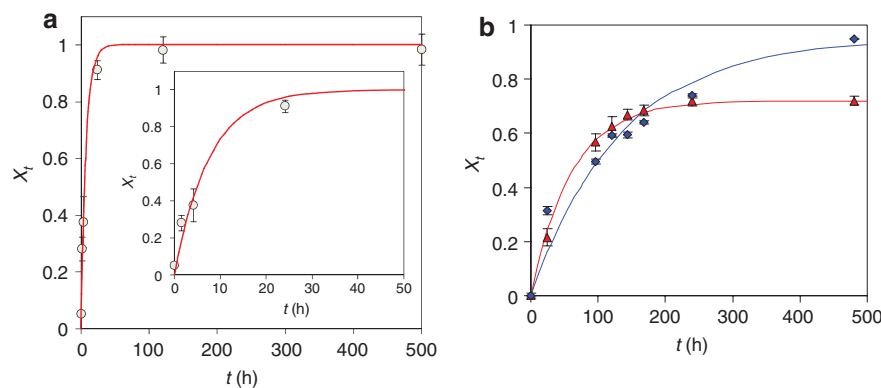


**Fig. 7:** Kinetics of nanolime carbonation in air and carbonate phases evolution. (a) experimental (circles) and calculated (model-fitting to a deceleratory F1 kinetic model; solid red curve) results for the carbonation of nanolime considering the full amount of calcium carbonate (amorphous and crystalline) determined using thermogravimetry. The inset shows a detail of the early stages of conversion; (b) Experimental results (symbols) and fitting (solid lines) to a deceleratory first-order kinetic model for vaterite-to-calcite conversion (red triangles/line) and aragonite-to-calcite conversion (blue rhombs/line). Reproduced from Rodriguez-Navarro et al. [95] with permission from The Royal Society of Chemistry.

analysis of crystalline calcium carbonate phases formed during carbonation. Note, however, that only calcite (band at  $712\text{ cm}^{-1}$ ) was considered, whereas the band at  $749\text{ cm}^{-1}$ , demonstrating the presence of abundant vaterite, was not. Baglioni et al. [42] showed that the carbonation of commercial nanolime involved an initial induction period. Rodriguez-Navarro et al. [95] showed that if only crystalline  $\text{CaCO}_3$  phases were considered, the carbonation kinetics could indeed be fitted to an Avrami-Erofeev model. However, if both amorphous and crystalline calcium carbonate phases were considered for the kinetic analysis, the system followed a deceleratory (pseudo)first order (F1) kinetic model of the type

$$X_t = X_{\max} (1 - \exp(-kt)) \quad (16)$$

where  $X_t$  and  $X_{\max}$  are the fractional amounts of  $\text{Ca}(\text{OH})_2$  converted into  $\text{CaCO}_3$  at time  $t$  and at maximum conversion, respectively. In this latter case, the induction time characteristic of the Avrami-Erofeev model was not observed (Fig. 7a). The same kinetic model was followed by the conversion of vaterite and aragonite into calcite [95] (Fig. 7b). Overall, these kinetic results showed that the carbonation of  $\text{Ca}(\text{OH})_2$  is a deceleratory process controlled by the  $t$ -evolution of reactant concentration.

## Applications of nanolimes

### Application methods

There are several precautions and application methods that can be implemented when nanolimes are used in conservation interventions on a range of substrates. Nanolime dispersions should be applied on dry surfaces [118]. Pre-treatment with the same alcohol used in the dispersion is advisable to dry the pores if the material is wet, which ensures a better penetration of the nanoparticles. Additionally, the existence of previous treatments with polymers and other organic materials might hamper nanoparticle penetration; thus, any coating should be removed before applying a consolidation treatment based on nanolimes [34]. After drying and coating removal, nanolime dispersions are usually applied by brushing with a flat brush over a Japanese paper sheet (Fig. 8). The use of Japanese paper is particularly recommended when nanolimes are applied as a pre-consolidation treatment on very delicate surfaces such as wall paintings [25, 53]. The Japanese paper sheet should adhere to the surface while pressed during brushing, and its pore size should be selected as to be higher than the maximum particle size of the nanolime dispersion [25]. If the relative humidity of the



**Fig. 8:** Example of the conservation of wall painting (archeological site of Ixcaquixtla) involving the application of nanolimes. On the left, salt crystallization has led to the powdering of the paint layer with a consequent loss of pigments. On the center, a conservator applies the treatment (note the use of Japanese paper). On the right, the same area after the conservation intervention. Reprinted from Chelazzi et al. [33]. Copyright (2013), with permission from Elsevier.

environment is lower than 70 %, the application of a cellulose poultice soaked with distilled water over the Japanese paper is recommended to prevent the formation of white hazes and to favor nanolime carbonation [34]. Once it is dried, the poultice and the Japanese paper can be removed. High nanoparticle concentrations, low porosities of the substrate, or too dry environments can result in the formation of white hazes and thus limit the penetration of the nanoparticles [118], in some cases due to back-migration of the nanoparticles [41]. Hazes can be removed by applying alcohol by brushing or with the above-mentioned cellulose poultice, or using a sponge [118].

Additionally, nanoparticles can be applied using a syringe. This method is preferred when the nanoparticles must be injected behind detached fragments that should be re-adhered, or to fill gaps or cracks, using highly concentrated dispersions [118]. If the surface mechanical resistance allows it, a light pressure can be applied during injection of the treatment; several injections may be needed to achieve consolidation after full carbonation of the particles [34]. Finally, in the case of highly deteriorated surfaces, nanolimes can also be sprayed on the surface using a nebulizer as a pre-consolidation treatment. The dispersions are sprayed on the surface of the painting until surface saturation using an aerosol sprayer held ca. 10 cm from the surface [34]. This method allows controlling the amount of material introduced into the substrate. Application by brush or syringe can produce bigger optical changes, and these methods are considered more suitable for more porous substrates. Other application methods include pouring, immersion, vacuum impregnation and systematic dripping techniques [94]. In the case of non-capillary active substrates the slow and gradual application of the consolidant is highly recommended. The extent of particles penetration depends largely on the substrate properties (pore size distribution, chemical composition, moisture content), on the environmental conditions (e.g.  $T$  or  $RH$ ) and on the solvent carrying the nanoparticles. Penetration lengths reported in the literature vary from hundreds of microns up to a few centimeters in the case of highly porous materials [34].

The uptake of product depends both on the applied nanoparticle concentration and on the properties of the substrate (such as porosity or presence of moisture within the pores). Typically, for wall painting consolidation, 1 L of product at a concentration of 5 g/L is needed to treat ca. 5–10 m<sup>2</sup> of a surface with a normal porosity and decohesion [34]. Overall, it can be said that the standard concentration of nanolime products such as Nanorestore® is 5 g/L. However, lower concentrations can be suitable for application on low porosity materials, depending as well on the degree of alteration of the substrate. For the consolidation of lime mortars, application of different concentrations (5 and 25 g/L in propan-2-ol) of different products (CaLoSiL®,

Nanorestore® and Merck®) showed that higher degrees of carbonation within the pores are achieved when lower concentrations (CaLoSiL® 5 g/L) are applied [119]. The more effective protective and consolidating action of diluted nanolime treatments compared to the undiluted ones has been confirmed as well on several natural stones [111]. Moreover, the application of an excess of product commonly results in the formation of undesired white hazes, which can be removed by applying a light spray of water. This can be avoided using dispersions with low concentration (from 1 to 3 g/L). In this way, aggregation of particles is reduced and nanoparticle penetration is enhanced [34].

As a general rule, better results are achieved when the nanolime suspension is applied several times (up to 10) at lower concentrations. However, the optimal concentration and number of applications ultimately depend on the stone porosity and pore size; tests performed using CaLoSiL® with different concentrations on stones with coarse pores showed that the optimal treatment in this case was two applications of CaLoSiL® at 25 g/L [120]. Depending on the substrate porosity and degradation status, it is also possible to apply dispersions of different concentrations, starting from the lower concentration up to the higher [118].

As stated above, nanoparticles dispersed in short-chain alcohols are much more stable than suspensions in water [25]; they penetrate deeper into porous structures and carbonate faster because of their lower degree of agglomeration and higher surface area [121]; they allow higher calcium hydroxide concentration, thus introducing more nanoparticles into the treated substrate [83]; and they reduce the amount of water introduced into the substrate. For practical conservation applications, nanolime suspensions are prepared in ethanol, propan-2-ol and propan-1-ol. Those in ethanol have a slightly lower viscosity. The effect of the solvent on the penetration depth of the suspensions has been recently studied [41]. Solvents with high boiling points improve the penetration depth of nanolime treatments in stones with large pores (35–40 µm), while solvents with lower boiling points perform better in materials with smaller pore size (0.5–2 µm). Nonetheless, ethanol nanolime dispersions applied on highly porous Maastricht limestone, which is characterized by coarse pores, led to significant consolidation (measured using a drilling resistance measurement system, DRMS) up to a remarkable depth of ~16 mm [122]. In general, nanolimes dispersed in ethanol seem to be more effective consolidants than nanolimes in propan-2-ol [94]. Test results clearly show that CaLoSiL® E-25 (E stands for ethanol, and 25 for a nanoparticle concentration of 25 g/L) gives higher increases in compressive strength than CaLoSiL® IP-25 or E-50 (IP stands for propan-2-ol, while 50 refers to a nanoparticle concentration of 50 g/L) for consolidation of limestones. The percentage increase in tensile strength, however, was lower with E-25 than IP-25. As propan-2-ol does not penetrate as deeply as ethanol due to its higher molecular weight, higher concentrations of nanoparticles were found near the surface when they were applied dispersed in propan-2-ol compared to ethanol. It has been experimentally found that when a consolidant distributes more homogeneously within a substrate, improved compressive strengths are achieved, whereas if the consolidant accumulates near the surface, the tensile strength increases. Related to its lower penetrability compared to ethanol, white deposits on the material surface are more commonly observed when using nanolime dispersed in propan-2-ol [94]. Additionally, a deeper penetration of the treatment reduces nanolime migration back to the surface during drying of the solvent [41].

## Nanoparticles for conservation of lime-based artifacts and stone

Since 2000, nanolime dispersions have been tested as potential consolidation treatments for substrates as varied as wall paintings, limestone, lime mortars, renders and plasters, and on the deacidification of cellulose materials such as paper, canvas and wood. The use of nanoparticles in consolidation treatments as an alternative to conventional polymeric treatments was first tested in wall paintings. The decay of wall paintings made with slaked lime according to the fresco technique commonly results in flaking and powdering of the painted surface, as a result of the loss of the carbonate binder [31]. Applied Ca(OH)<sub>2</sub> nanoparticles replace the lost binder, consolidating the painting in a fully compatible way. As indicated in the Introduction section, the use of calcium hydroxide nanoparticle dispersions in short-chain aliphatic alcohols (such as propan-1-ol) as a consolidation treatment for wall paintings was first reported by Giorgi and co-workers [25], who obtained better

results than with aqueous solutions or dispersions and less superficial white hazes. These nanolime dispersions were applied in the treatment of wall paintings in Santa Maria Novella in Florence, by brushing through Japanese tissue. Later, Ambrosi and co-workers [71] used  $\text{Ca}(\text{OH})_2$  nanoparticles in the restoration of Santi di Tito's wall paintings (16<sup>th</sup> century) in the Santa Maria del Fiore Cathedral in Florence with excellent results (Fig. 9). Since then, nanolimes have been tested on other Italian frescoes (see for example [31, 83]), producing positive results in terms of color and re-aggregation of the flakes of pigment. Researchers of the same group also explored the performance of propan-2-ol dispersions, for example on wall paintings at the Museo del Bargello, where they focused on the study of color stability, and in the church of Santa Croce, both located in Florence (see D'Armada and Hirst [94] and refs. therein). Outside of Europe, this nanoparticle technology has been also successfully applied to the conservation of stucco and paints in the UNESCO World Heritage Site of Calakmul in the Yucatan peninsula (Mexico) [123, 124]. After treatment with nanoparticles [124], testing of the resistance to abrasion indicated complete fixation of color in damaged paintings [16]. Overall, these studies have demonstrated that nanolime treatments are among the best for wall painting consolidation.

There are numerous examples of the application of nanolime suspensions on stone, specially limestone. One of the first reports on the use of nanolimes for stone consolidation is the work by Ambrosi et al. [72], who applied  $\text{Ca}(\text{OH})_2$  suspensions prepared in propan-1-ol to carbonatic stones showing flaking and powdering from architectonic sites in Rome and near Padua. Scotch tape tests performed after the application of

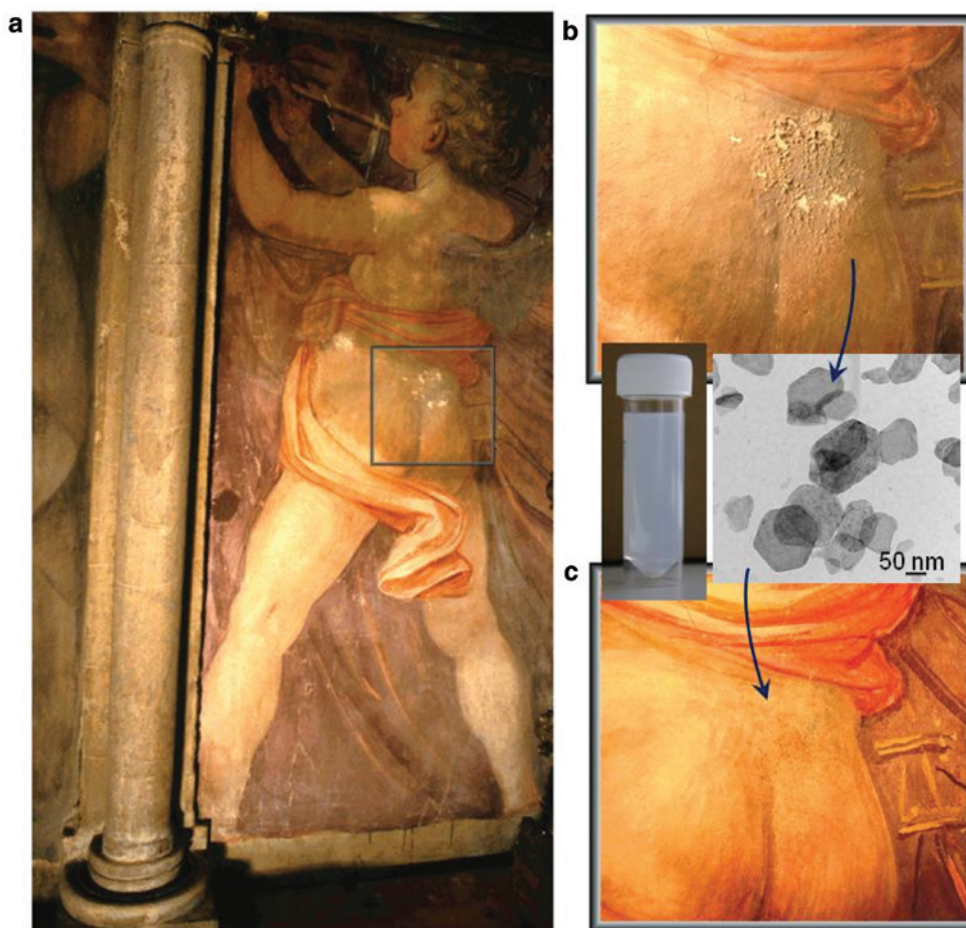


**Fig. 9:** Example of nanolime application (insets show a nanolime dispersion and a TEM image of nanolime particles) during the preconsolidation of the wall paintings by Santi di Tito (16<sup>th</sup> century) *Gli Angeli Musicanti* on the Counterfaçade of the Santa Maria del Fiore Cathedral in Florence, Italy. The squared area in (a) is that treated with the nanoparticles: (b) before the restoration and (c) after the restoration. Adapted with permission from Ambrosi et al. [71]. Copyright (2001) American Chemical Society.

the suspensions demonstrated the reinforcement of stone superficial cohesion. However, the penetration depth of the treatment was not reported. Later on, Dei and Salvadori [83] showed that the application of nanosized calcium hydroxide particles has positive consolidating effects on low-porosity limestones, both at the surface of the material (re-aggregating the powdering surfaces) and inside the stone matrix (decreasing its tendency to absorb water). The effective consolidating and protective action of these treatments on two natural stones (Estoril and Pietra Serena) has been as well reported by Daniele et al. [75]. Three different tests seem to confirm the protective and consolidating effectiveness of the treatment: “Scotch Tape Test”, capillarity and imbibition tests.

Nanolimes have been also used for the consolidation of dolostones. López-Arce et al. [108] indicated that the treatment improved the physical and hydric properties of the stone specimens following carbonation in dry (33 % RH) and humid (75 % RH) environments. Additional studies indicated that nanolime dispersions in propan-2-ol (2 g/L) applied in a humid environment (75 % RH) contributed to an increase in the ultrasound velocity and density of dolostones, without significantly changing the stone color and brightness [125]. Alkaline-earth metal hydroxide nanoparticles dispersed in alcohol have been applied onto “Pietra d’Angera”, a dolostone that is commonly affected by freeze–thaw cycles and acid rain, as well as past consolidation treatments (e.g. use of cement or polymers). Although dispersions of lime nanoparticles are considered to be efficient at preserving dolostone surfaces [33], there are some potential drawbacks of the interaction between  $\text{Ca}(\text{OH})_2$  and dolomite [ $\text{CaMg}(\text{CO}_3)_2$ ] that need to be considered (see below).

Compared to “traditional” consolidants such as TEOS or polymers, nanolime treatments have demonstrated similar or better performance when applied to consolidate carbonate stones [117, 126]. Carretti and co-workers [117] performed a comparative study on the effect of different consolidation treatments based on the application of  $\text{Ca}(\text{OH})_2$  nanoparticles and polymers on three different types of carbonate stones: Maas-tricht limestone, travertine, and Carrara marble. Scotch tape tests showed that  $\text{Ca}(\text{OH})_2$  dispersions gave the best performance in terms of recovery of mechanical properties, without affecting water vapor permeability. Similar conclusions were obtained upon application of alkaline-earth metal hydroxide nanoparticle suspensions on highly porous stones (Lecce stone). Improved formulations of nanolime suspensions used for the consolidation of stones include the addition of surfactants. Standard tests performed on carbonatic natural stones upon application of surfactant-bearing suspensions seem to confirm their consolidating effect, particularly in highly porous stones such as travertine [78].

There are also some case studies where nanolime dispersions were reported to be successfully applied on a range of non-calcareous stone substrates such as tuff, sandstone and trachyte [118]. In the case of sandstones (e.g. Rotliegend-sandstone at the church of St. Mauritius in Tholey, Germany), best results were observed when combining the application of nanolime and alkoxy-silanes [127]. Rodriguez-Navarro et al. [27] observed an effective consolidation of Prague sandstone following application of different alcohol dispersions of both commercial nanolime (Nanorestore<sup>®</sup>, 5 g/L) and non-commercial propan-2-ol dispersions of  $\text{Ca}(\text{OH})_2$  particles (5 g/L) from aged lime putty and carbide lime putty. The degree of consolidation reached after treatment application was evaluated by measuring the weight loss following sonication tests. Best results were obtained when using aged lime putty dispersions. This is likely due to the fact that the lime putties had both nano- and micrometer sized portlandite particles, which optimally deposited in the coarse pores (~10  $\mu\text{m}$ ) of the sandstone. This is consistent with the statement by Borsoi et al. [41] indicating that in the case of limestones with coarse pores, the presence of portlandite particles of relatively coarse size is beneficial, as such particles are less prone to back migration during solvent evaporation.

Nanolime dispersions have been as well tested as a potential consolidation treatment for mortars. Using CaLoSiL<sup>®</sup>, Drdácý et al. [23] documented a significant increase in strength in lime mortars with far fewer applications than with limewater. Studies performed by Borsoi et al. [122, 128, 129] concluded that the treatment with nanolime dispersions permits a homogeneous distribution and optimum penetration of the consolidant within lime mortars, achieving a significant consolidation up to a depth of 6–8 mm, according to DRMS results [122]. A recent comparative study of different commercial nanolime dispersions (CaLoSiL<sup>®</sup>, Nanorestore<sup>®</sup> and Merck<sup>®</sup>) showed that CaLoSiL<sup>®</sup> at 5 g/L produced the most significant improvement in the degree of carbonation and in compactness of the mortar, due to the precipitation of calcite and aragonite

within the pores between the matrix and the aggregate [119]. This product also caused the least significant chromatic changes and the greatest increase in ultrasonic propagation velocity. Nanolimes have also been tested on Portland cement mortars, showing as well an increase in the mechanical strength after treatment, with limited effect on the pore system, color or surfaces properties [130]. To our knowledge, however, few studies have evaluated the performance of nanolime suspensions as a potential consolidation treatment for non-calcareous clay-based artifacts, such as bricks and ceramics, or adobe. Ambrosi et al. [72] applied nanolime dispersions on bricks of the external walls of the Santa Prisca in Aventino (Rome, Italy), indicating that the results of the treatment were fair. Nonetheless, a penetration depth of  $<0.5$  mm was observed. In this respect, Costa and co-workers [131] did not find significant evidence of nanolimes inducing any increase in the original hardness of ceramic (azulejo) materials. Conversely, Lanzon et al. [132] have reported a significant surface consolidation in adobe bricks following application of diluted propyl-2-ol nanolime dispersions (applied by spraying).

## Applications on organic materials

In addition to their use as consolidants for the different inorganic artifacts described above, calcium and also magnesium hydroxides have proven to be excellent compounds for the deacidification of cellulosic works of art. Cellulose-based artifacts experience hydrolysis and oxidation reactions that result in the loss of the mechanical resistance of the fibers and discoloration [52]. The use of non-aqueous solvents for the treatment of these materials avoids alkaline depolymerization of cellulose and decomposition of water-sensitive paper components, such as inks and sizing. Nanolime dispersions can be applied to paper or canvas using conventional procedures.  $\text{Ca}(\text{OH})_2$  nanoparticles suspended in propan-1-ol produce safe and stable deacidification of cellulose-based artifacts and react with carbon dioxide from the air, forming a calcium carbonate deposit on the paper fibers that acts as a buffer against reoccurring acidity, thus enabling the long-term control of paper pH (see Baglioni et al. [52] and Refs. therein). Deacidification of 14<sup>th</sup>, 17<sup>th</sup>, 19<sup>th</sup>, and 20<sup>th</sup> century acid yellowed paper samples has been successfully performed [54]. Additionally, samples of paper from the 18<sup>th</sup> century have been treated with  $\text{Mg}(\text{OH})_2$  nanoparticles and subsequently aged by hydrothermal and photooxidative degradation. The nanoparticle treatment was found to significantly maintain the mechanical features of paper, and its deterioration was greatly reduced [74]. More recently, Poggi et al. [68] applied calcium hydroxide nanoparticles dispersed in ethanol and propan-2-ol to acidic paper and canvas samples, and they found that their degradation rate was significantly reduced in deacidified samples. The results of these works indicate that application of nanoparticle dispersions is a valid treatment for the conservation of cellulose-based works of art, and opens new ways for the preservation of materials such as parchment and leather.

Ca and Mg hydroxide nanoparticles dispersed in alcohols have proven to be also efficient for the deacidification of archeological wood. Their performance has been investigated in the context of the preservation of the Swedish 17<sup>th</sup> century warship Vasa [133], whose timbers contain high quantities of sulfuric acid [69, 74, 134] (Fig. 10). The studies performed on this material show that wood from the Vasa warship can be effectively deacidified by using a  $\text{Ca}(\text{OH})_2$  dispersion in propan-2-ol. This nanoparticle dispersion can homogeneously penetrate inside the wood up to 20 cm, neutralizing acidity and creating an alkaline buffer inside the wooden matrix, which prevents the degradation of residual cellulose (Fig. 10). Alkaline nanoparticles react with the acid present in the wood and are converted into calcium sulfate without mechanical stress. The excess calcium hydroxide nanoparticles are converted into calcium carbonate, which acts as a buffer that protects the wood from future acid attack. Artificial aging tests performed on Vasa wood have demonstrated that nanoparticles protect wood towards further acid degradation [69, 74, 134]. Similarly,  $\text{Ca}(\text{OH})_2$  (or  $\text{Mg}(\text{OH})_2$ ) nanoparticle dispersions have been successfully applied to decrease the emissions of organic acid vapors associated with wood acidification in ancient organs [76]. Such VOCs corrode the lead pipes of ancient organs. Upon nanolime application, the emission of VOCs was demonstrated to be significantly reduced.

Additionally, combined treatments using propylene glycol modified TEOS and alkaline nanoparticles ( $\text{Ca}(\text{OH})_2$ ) have been recently applied to the wooden objects from the Oseberg find [135], which were

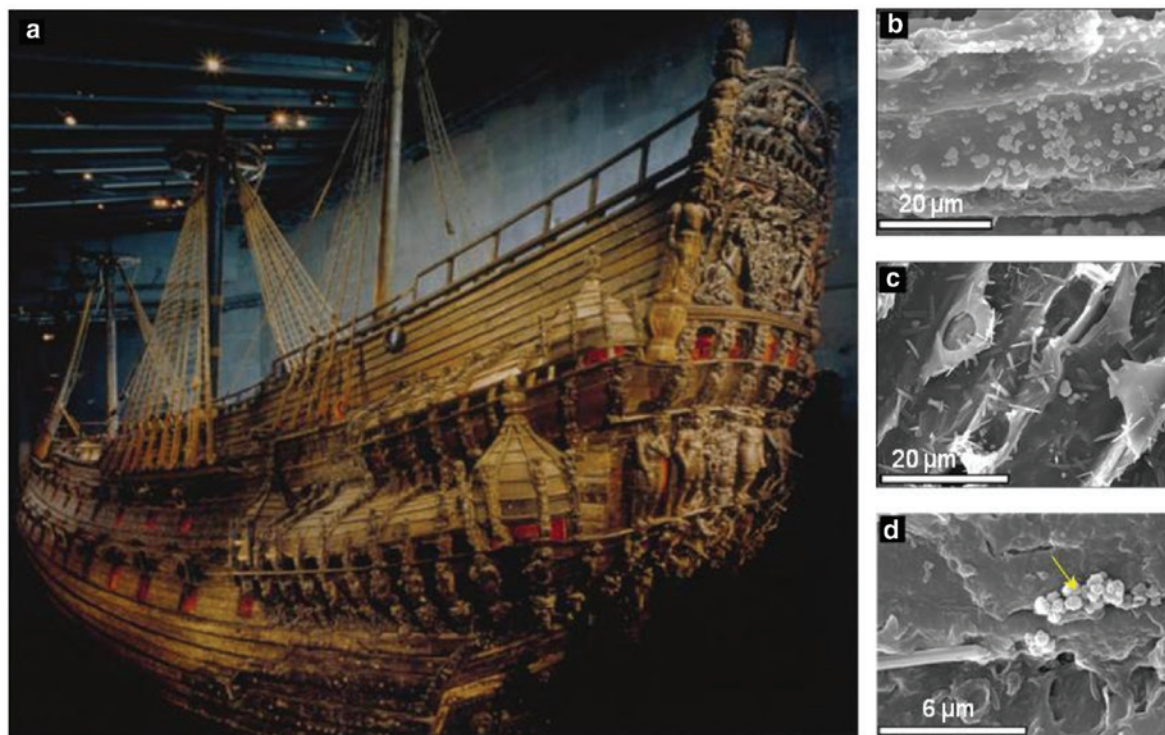


**Fig. 10:** The Vasa warship at the Vasa Museum, Stockholm. (a) General overview of the Vasa warship, which was affected by extensive acidification due to  $\text{H}_2\text{SO}_4$  formation; (b) SEM photomicrographs of Vasa warship wood after treatment with nanolime. The  $\text{Ca}(\text{OH})_2$  nanoparticles are observed on the wall fibers of wood, 1.5 cm below the wood surface; (c) fibrous gypsum crystals formed after deacidification; (d) calcium carbonate (arrow) alkaline reservoir. Panel (a) reprinted by permission from Macmillan Publishers Ltd: Nature (Gillon [133]), copyright (2002); Panels (b–d) adapted with permission from Giorgi et al. [74]. Copyright (2005) American Chemical Society.

deteriorated due to previous conservation treatments based on alum salts. As a consequence of these treatments, the artifacts were highly fragile; in some cases wood had almost completely lost its structural integrity. Treatment of these archeological wooden objects with a combination of alkaline nanoparticles and propylene glycol modified silane (PGMS) monomers resulted in enhanced robustness and increased pH of the wood.

### Limitations of nanolime treatments

Although the potential of nanolime dispersions for surface consolidation has been undoubtedly evidenced by the numerous studies performed in the last two decades, when bulk consolidation is needed, their efficiency is still under debate (see Borsoi et al. [41] and Refs. therein). For instance, Campbell et al. [136] showed that the consolidation of Portland limestone using a commercial nanolime ( $\text{CaLoSiL}^{\text{®}}$ ) led to a slight decrease in sorptivity without pore blocking, which was considered a positive effect. However, drilling resistance and scratch tests showed no detectable improvement of the mechanical properties. In this case, as in others where no detectable consolidation effect was detected, one of the reasons of the limited effectiveness of these treatments is the accumulation of nanoparticles at or just below the surface (<1 mm deep), resulting in some cases in the formation of a white deposit. It could be argued that this might be due to coagulation of the nanoparticles, resulting in larger aggregates that would not penetrate within micrometer-sized pores typically present in stone or plaster. However, pigment particles (~300 nm in size) larger than typical nanolime particles, have been shown to be able to penetrate centimeters into a limestone with pores <10  $\mu\text{m}$  [137]. It follows that coarsening due to coagulation is not a likely explanation for the poor penetration of nanolimes observed in some cases. Apparently, surface accumulation occurs during the drying phase

rather than during absorption, when the solvent moves back to the surface, depositing a significant amount of the nanolime particles [41]. To avoid this effect, solvents with slower drying rate, higher boiling points (water or butanol) and higher dielectric constant or even water/alcohol binary mixtures might be used [41, 138]; this favors nanoparticle/solvent phase separation and results in a more homogeneous distribution of lime nanoparticles in depth, especially in the case of stones with coarse pores [41, 138]. Additionally, optimization of application strategies may help achieving a more homogenous deposition of nanolime particles within the substrate.

Another drawback of the use of nanolimes is that once dispersed in short-chain alcohols they can undergo transformation into calcium alkoxides [27, 113]. Ca-alkoxides significantly reduce the rate of carbonation of the nanoparticles and induce the formation of metastable vaterite, as opposed to stable calcite formed in untransformed  $\text{Ca}(\text{OH})_2$  samples [113]. Such effects may hamper/delay the strengthening or consolidation effects of nanolimes. Moreover, it has been reported that commercial nanolimes applied onto non-carbonate porous substrates (such as sandstones) show a lower consolidation efficiency than propan-2-ol dispersions of aged slaked lime putty, in spite of the faster and more extensive carbonation achieved in the case of commercial nanolimes [27]. This has been related to the formation in the former case of metastable vaterite as the cementing carbonate phase due to the presence of calcium alkoxide after the partial conversion of nanolime (due to long term -months- storage of the commercial nanolime dispersion prior to application), while stable calcite was formed in the case of aged slaked lime dispersions where only pure  $\text{Ca}(\text{OH})_2$  was present [27].

Another potential drawback of the use of  $\text{Ca}(\text{OH})_2$  nanolime dispersions refers to their application on dolostones. Nanolimes have been applied for the consolidation of Redueña dolostones, a type of carbonate stone profusely used in the built heritage of Madrid (Spain) and surrounding areas [108]. Commercial nanolimes with a concentration of  $\text{Ca}(\text{OH})_2$  nanoparticles of 5 g/L dispersed in propan-2-ol (Nanorestore<sup>®</sup>) were applied on dolostone specimens. Analysis of the treated samples using ESEM and surface profilometry revealed the dissolution and fracturing of dolomite crystals, and the subsequent re-crystallization of calcite. Apparently, this occurs by means of the well-known alkali-dolomite reaction [139]



The problem with this reaction is that the resulting  $\text{Mg}(\text{OH})_2$  is more soluble than both calcite and dolomite (i.e. can be leached in contact with aqueous solutions) and has a very low carbonation rate, which may hamper consolidation in the short term. In the long term, the carbonation of  $\text{Mg}(\text{OH})_2$  will not result in the precipitation of a stable  $\text{MgCO}_3$  cement. This is due to the fact that magnesite (and dolomite) can not easily precipitate at STP conditions due to the high hydration energy of  $\text{Mg}^{2+}$  ions [140]. Instead, a series of hydrous magnesium carbonate phases, such as nesquehonite, lansfordite and/or hydromagnesite, will form. These phases are moderately soluble, and do not seem to provide any effective consolidation. Indeed, López-Arce et al. [108] showed that in some cases, dolostone specimens showed a higher amount of water absorption (by capillarity) after nanolime treatment, an effect that can be explained by the dissolution of the dolostone via reaction (17) resulting in a porosity increase.

Despite the numerous advantages of nanolimes as a consolidation treatment (high stability, fast carbonation rate and a generally good chemical and physical compatibility with calcareous stone and lime-based plasters), its penetration depth is frequently lower than that achieved by TEOS-based consolidants, which may consequently result in limited consolidation when only nanolime treatments are used [41]. Therefore, for an improved consolidation treatment there is commonly the need to combine nanolime treatments with conventional consolidants (e.g. ethyl silicates). In this respect, Ziegenbalg [118] indicates that an effective treatment strategy involves the initial application of a nanolime dispersion, followed by the application of TEOS. The high pH associated with the nanolime particles promotes the alkaline hydrolysis of the alkoxysilane, resulting in a more effective consolidation via the formation of a silica gel. Moreover, the presence of the nanolime seems to favor a better bonding between the silica coating and the substrate in the case of carbonate-based materials such as limestone or lime mortars.

Finally, it is necessary to briefly address the potential health/safety and environmental risks that the use of  $\text{Ca}(\text{OH})_2$  nanoparticles dispersed in alcohol can pose. On the one hand, and regarding the  $\text{Ca}(\text{OH})_2$



nanoparticles, other than the necessary precautions required when handling a strong base (e.g. to prevent skin irritation), no cytotoxic or other health-related risks have been detected [141]. On the other hand, the use of alcohols as solvents might be considered a handicap under increasingly stringent safety and environmental regulations. Ethanol, propan-1-ol, and propan-2-ol are all flammable, so necessary precautions should be taken, especially during application and early evaporation. The three alcohols are, however, low-toxicity VOCs under both EU and USA regulations. Indeed, the above-mentioned short-chain alcohols can be considered as much less hazardous than most common VOCs used as solvents, as it is the case of petroleum-derived VOCs such as white spirit. Nonetheless, their contact with the skin and their inhalation during treatment application should be carefully controlled, as should be their release to the environment. From a health-related perspective, ethanol should be the solvent of choice due to its lower toxicity compared with propan-2-ol or propan-1-ol.

## Summary and outlook

The works reviewed here clearly show that alkaline-earth metal hydroxides (calcium, magnesium, barium and strontium hydroxide) nanoparticle suspensions in short-chain alcohols are effective tools for tackling the degradation processes affecting cultural heritage objects and structures, without altering the physical–chemical properties of the treated works of art. Practical applications to stone, wall paintings, paper and wood, among other materials, show that nanolime dispersions, being physically and chemically compatible with materials used in cultural heritage, show similar or better performance than conventional treatments (i.e. polymers, alkoxy silanes or limewater). Moreover, they do not require a special application method, and can be applied by brushing, spraying, injection, pouring, immersion, vacuum impregnation or systematic dripping techniques.

Since the first works performed at the end of the past century and early this century, considerable effort has been devoted to advance in the optimization of the synthesis methods of these nanoparticle suspensions (lime slaking, sol–gel and solvothermal synthesis, aqueous homogeneous precipitation routes, synthesis in diols, use of W/O microemulsions, ion exchange resins or insolubilization-precipitation) and their application in the field of heritage conservation. The carbonation reaction upon alcohol evaporation and contact with atmospheric  $\text{CO}_2$ , is the main mechanism responsible for the consolidation effect of nanolimes. Moreover, the precipitated  $\text{CaCO}_3$  acts a pH buffer in deacidification treatments of wood and paper. The ambient relative humidity (RH) is a key parameter affecting the carbonation kinetics of nanolimes, with faster and more extensive carbonation observed in the RH range from 33 % up to 95 %. The carbonation rate is of paramount importance for a fast and effective consolidation of the damaged substrate using nanolime suspensions.

Although it is now clear that nanolimes are fundamental tools for the consolidation of porous substrates, and despite the fast increase in the number of studies on nanolime as a conservation material, research in this field is still far from being completed. In this sense, research efforts should focus on improving the effectiveness of nanolime dispersions for bulk consolidation, and, in particular, on (i) achieving a homogenous deposition of nanolime particles in the interior of the substrate and (ii) the optimization of combined treatments using nanolimes and conventional consolidants (e.g. ethyl silicates), which may help to fully extend the application of nanolime treatments to non-calcareous (i.e. silicate) substrates.

Finally, although short-chain aliphatic alcohols used as dispersion media in nanolimes are considered to pose a low health risk, the use of alternative, more health- and environmentally-friendly solvents should be explored (e.g. green solvents). Furthermore, systems aimed at capturing in situ these volatile organic solvents following nanolime application need to be developed.

**Acknowledgements:** This research was funded by the Spanish Government (grant CGL2015-70642-R) and the Junta de Andalucía (grant P11-RNM-7550). Additional funding from the research group RNM-179 of the Junta de Andalucía and the Unidad Científica de Excelencia UCE-2016-05 of the University of Granada is acknowledged.

## References

- [1] C. Rodríguez-Navarro, E. Sebastian. *Sci. Total Environm.* **187**, 79 (1996).
- [2] E. Winkler. *Stone in Architecture: Properties, Durability* (3rd edition), Springer, Berlin (1997).
- [3] T. Warscheid, J. Braams. *Int. Biodet. Biodegr.* **46**, 343 (2000).
- [4] I. Jiménez-González, C. Rodríguez-Navarro, G. W. Scherer. *J. Geophys. Res. Earth Surf.* **113**, F02021 (2008).
- [5] E. Doehne, C. A. Price. *Stone Conservation: An Overview of Current Research*, Getty Conservation Institute, Los Angeles (2010).
- [6] M. Schiro, E. Ruiz-Agudo, C. Rodríguez-Navarro. *Phys. Rev. Lett.* **109**, 265503 (2012).
- [7] V. Vergès-Belmin (ed.). *Illustrated Glossary on Stone Deterioration Patterns*, ICOMOS International Scientific Committee for Stone, Charenton-le-Pont (2008).
- [8] L. Lazzarini, M. L. Tabasso. *Il Restauro della Pietra*, Cedom, Milan (1986).
- [9] C. Selwitz. *Epoxy Resins in Stone Conservation*, Getty Conservation Institute, Los Angeles (1992).
- [10] G. W. Scherer, G. S. Wheeler. *Key Eng. Mater.* **391**, 1 (2009).
- [11] S. Z. Lewin, N. S. Baer. *Studies Conservation* **19**, 24 (1974).
- [12] A. Burgos-Cara, E. Ruiz-Agudo, C. Rodríguez-Navarro. *Mater. Design* **115**, 82 (2017).
- [13] E. Sassoni, S. Naidu, G. W. Scherer. *J. Cult. Herit.* **12**, 346 (2011).
- [14] M. Favaro, P. Tomasin, F. Ossola, P. A. Vigato. *Appl. Organometal. Chem.* **22**, 698 (2008).
- [15] F. Jroundi, M. Schiro, E. Ruiz-Agudo, K. Elert, I. Martín-Sánchez, M. T. González-Muñoz, C. Rodríguez-Navarro. *Nature Commun.* **8**, 279 (2017).
- [16] P. Baglioni, R. Giorgi, L. Dei. *Compt. Rend. Chim.* **12**, 61 (2009).
- [17] R. Giorgi, M. Baglioni, D. Berti, P. Baglioni. *Accounts Chem. Res.* **43**, 695 (2010).
- [18] M. Favaro, R. Mendichi, F. Ossola, U. Russo, S. Simon, P. Tomasin, P. A. Vigato. *Polym. Degrad. Stability* **91**, 3083 (2006).
- [19] E. Hansen, E. Doehne, J. Fidler, J. Larson, B. Martin, M. Matteini, C. Rodríguez-Navarro, E. Sebastián Pardo, C. Price, A. de Tagle, J. M. Teutonico, N. Weiss. *Rev. Conservation* **4**, 13 (2003).
- [20] J. Ashurst, N. Ashurst. *Practical Building Conservation. Vol. 1. Stone Masonry*, Halsted Press, New York (1988).
- [21] T. Quayle. *Conservation News* **59**, 68 (1996).
- [22] R. S. Boynton. *Chemistry and Technology of Lime and Limestone*, Wiley, New York (1980).
- [23] M. Drdáccký, Z. Slížková, G. Ziegenbalg. *J. Nano Res.* **8**, 13 (2009).
- [24] C. Price, K. Ross, G. White. *Studies Conservation* **33**, 178 (1988).
- [25] R. Giorgi, L. Dei, P. Baglioni. *Studies Conservation* **45**, 154 (2000).
- [26] P. Baglioni, L. Dei, E. Ferroni, R. Giorgi. *Patent T1286868 (B1)* (Priority date: 1996-10-31) (1998).
- [27] C. Rodríguez-Navarro, A. Suzuki, E. Ruiz-Agudo. *Langmuir* **29**, 11457 (2013).
- [28] C. Rodríguez-Navarro, E. Ruiz-Agudo, M. Ortega-Huertas, E. Hansen. *Langmuir*, **21**, 10948 (2005).
- [29] P. Baglioni, L. Dei, R. Giorgi, C. V. Schettino. *Patent US2005042380 (A1)* (Priority date: 2002-01-15) (2005).
- [30] P. Baglioni, L. Dei, L. Fratoni, P. Lo Nosotro, M. Moroni. *Patent US2005175530 (A1)* (Priority date: 2002-03-28) (2005).
- [31] P. Baglioni, R. Giorgi, *Soft Matter* **2**, 293 (2006).
- [32] R. Giorgi, M. Ambrosi, N. Toccafondi, P. Baglioni. *Chem. Eur. J.* **16**, 9374 (2010).
- [33] D. Chelazzi, G. Poggi, Y. Jaidar, N. Toccafondi, R. Giorgi, P. Baglioni. *J. Colloid Interface Sci.* **392**, 42 (2013).
- [34] P. Baglioni, D. Chelazzi, R. Giorgi. *Nanotechnologies in the Conservation of Cultural Heritage: A Compendium of Materials and Techniques*, Springer, New York (2015).
- [35] K. Elert, C. Rodríguez-Navarro, E. Sebastian Pardo, E. Hansen, O. Cazalla, *Studies Conservation* **47**, 62 (2002).
- [36] D. W. Kingery, P. B. Vandiver, M. Prickett. *J. Field Archaeol.* **15**, 219 (1988).
- [37] C. Rodríguez-Navarro, E. Ruiz-Agudo, A. Luque, A. B. Rodríguez-Navarro, M. Ortega-Huertas. *Am. Mineral.* **94**, 578 (2009).
- [38] C. Rodríguez-Navarro, K. Kudłacz, E. Ruiz-Agudo. *Am. Mineral.* **97**, 38 (2012).
- [39] E. Ruiz-Agudo, C. Rodríguez-Navarro. *Langmuir* **26**, 3868 (2009).
- [40] K. Kudłacz, C. Rodríguez-Navarro. *Environm. Sci. Technol.* **48**, 12411 (2014).
- [41] G. Borsoi, B. Lubelli, R. van Hees, R. Veiga, A. S. Silva, L. Colla, L. Fedelle, P. Tomasin, *Colloids Surf. A: Physicochem. Eng. Aspects* **497**, 171 (2016).
- [42] P. Baglioni, D. Chelazzi, R. Giorgi, E. Carretti, N. Toccafondi, Y. Jaidar. *Appl. Phys. A* **114**, 723 (2014).
- [43] O. Cazalla, C. Rodríguez-Navarro, E. Sebastian, G. Cultrone, M. J. de la Torre. *J. Am. Ceram. Soc.* **83**, 1070 (2000).
- [44] C. Rodríguez-Navarro, E. Hansen, W. S. Ginell. *J. Am. Ceram. Soc.* **81**, 3032 (1998).
- [45] A. D. Cowper. *Lime and Lime Mortars*, Building Research Establishment, London (1927) (reprinted by Downhead, London, 1998).
- [46] C. Atzeni, A. Farci, D. Floris, P. Meloni. *J. Am. Ceram. Soc.* **87**, 1764 (2004).
- [47] M. A. Bermejo Sotillo, C. Rodríguez-Navarro, E. Ruiz-Agudo, K. Elert. *Patent US9034100* (priority date 04.05.2010) (2015).
- [48] D. A. Kirchgessner, M. J. Lorrain. *Ind. Eng. Chem. Res.* **26**, 2397 (1987).
- [49] R. J. Lee, C. Hsia, L.-S. Fan, *AIChE J.* **41**, 435 (1995).
- [50] J. Adanez, V. Fierro, F. García-Labiano, J. Palacios. *Fuel* **76**, 257 (1997).

- [51] H. G. Shin, H. Kim, Y. N. Kim, H. S. Lee. *Curr. Appl. Phys.* **9**, S276 (2009).
- [52] P. Baglioni, D. Chelazzi, R. Giorgi, G. Poggi. *Langmuir* **29**, 5110 (2013).
- [53] M. Natali, L. Saladino, F. Andriulo, D. C. Martino, E. Caponetti, E. Carretti, L. Dei. *J. Cult. Herit.* **15**, 151 (2014).
- [54] R. Giorgi, L. Dei, M. Ceccato, C. V. Schettino, P. Baglioni. *Langmuir* **18**, 8198 (2002).
- [55] G. Ziegenbalg. *Patent DE:10327514 B3* (priority date 17.06.2003) (2005).
- [56] F. M. Perkin, L. Pratt, *J. Chem. Soc. Trans.* **95**, 159 (1909).
- [57] R. C. Mehrotra. *J. Non-Cryst. Solids* **100**, 1 (1988).
- [58] G. Ziegenbalg. in *Proc. 11th Int. Congr. Deterioration and Conservation of Stone*, J. W. Lukaszewicz, P. Niemcewicz (Eds.), pp. 1109–1115. Nicolaus Copernicus University, Torun, Poland (2008).
- [59] G. Ziegenbalg, K. Brümmer, J. Pianski. in *Proc. 2nd Historic Mortars Conference HMC2010 and RILEM TC 203-RHM Final Workshop*, J. Valek, C. Groot, J. J. Huges (Eds.), pp. 1301–1309, RILEM Publications S.A.R.L., Prague (2010).
- [60] G. Ziegenbalg, M. Dobrzyńska-Musiela. in *Proc. Euro-American Congress REHABEND 2016*, L. Villegas, J. M. Manso (Eds.), pp. 1–12, Universidad de Cantabria, Santander (2016).
- [61] C. Rodríguez-Navarro, E. Ruiz-Agudo, J. Harris, S. E. Wolf. *J. Struct. Biol.* **196**, 260 (2016).
- [62] Y. Arai. *Chemistry of Powder Production*, Chapman & Hall, London (1996).
- [63] E. Fratini, M. G. Page, R. Giorgi, H. Cölfen, P. Baglioni, B. Demé, T. Zemb. *Langmuir* **23**, 2330 (2007).
- [64] A. Blee, J. G. Matison. *Mater. Forum* **32**, 121 (2008).
- [65] O. B. Koper, I. Lagadic, A. Volodin, K. J. Klabunde. *Chem. Mater.* **9**, 2468 (1997).
- [66] S. Utamapanya, K. J. Klabunde, J. R. Schlup. *Chem. Mater.* **3**, 175 (1991).
- [67] J. Wittekind. *Restaurator* **15**, 189 (1994).
- [68] G. Poggi, N. Toccafondi, L. N. Melita, J. C. Knowles, L. Bozec, R. Giorgi, P. Baglioni. *Appl. Phys. A* **114**, 685 (2014).
- [69] G. Poggi, N. Toccafondi, D. Chelazzi, P. Canton, R. Giorgi, P. Baglioni, *J. Colloid Interface Sci.* **473**, 1 (2016).
- [70] T. Liu, Y. Zhu, X. Zhang, T. Zhang, X. Li. *Mater. Lett.* **64**, 2575 (2010).
- [71] M. Ambrosi, P. Baglioni, L. Dei, R. Giorgi, C. Neto. *Langmuir* **17**, 4251 (2001).
- [72] M. Ambrosi, L. Dei, R. Giorgi, C. Neto, P. Baglioni. *Trends Colloid Interface Sci.* **15**, 68 (2001).
- [73] T. Yasue, Y. Tsuchida, Y. Arai. *Gypsum Lime* **189**, 17 (1984).
- [74] R. Giorgi, D. Chelazzi, P. Baglioni. *Langmuir* **21**, 10743 (2005).
- [75] V. Daniele, G. Taglieri, R. Quaresima. *J. Cult. Herit.* **9**, 294 (2008).
- [76] R. Giorgi, D. Chelazzi, E. Fratini, S. Langer, A. Niklasson, M. Rådemar, J. E. Svensson, P. Baglioni. *J. Cult. Herit.* **10**, 206 (2009).
- [77] A. Samanta, D. K. Chanda, P. S. Das, J. Ghosh, A. K. Mukhopadhyay, A. Dey. *J. Am. Ceram. Soc.* **99**, 787 (2016).
- [78] V. Daniele, G. Taglieri. *J. Cult. Herit.* **13**, 40 (2012).
- [79] M. Darroudi, M. Bagherpour, H. A. Hosseini, M. Ebrahimi. *Ceram. Int.* **42**, 3816 (2016).
- [80] J. Xu, Q. H. Chen, Q. R. Qian. *Chem. Res. Chinese Universities* **20**, 229 (2004).
- [81] A. Pérez-Maqueda, L. Wang, E. Matijević. *Langmuir* **14**, 4397 (1998).
- [82] B. Salvadori, L. Dei. *Langmuir* **17**, 2371 (2001).
- [83] L. Dei, B. Salvadori. *J. Cult. Herit.* **7**, 110 (2006).
- [84] A. Roy, J. Bhattacharya. *IET Micro Nano Lett.* **5**, 131 (2010).
- [85] B. Delfort, M. Born, A. Chivé, L. Barré, *J. Colloid Interface Sci.* **189**, 151 (1997).
- [86] A. Nanni, L. Dei. *Langmuir* **19**, 933 (2003).
- [87] G. Taglieri, V. Daniele, G. Del Re, R. Volpe, *Adv. Nanoparticles* **4**, 17 (2015).
- [88] G. Taglieri, V. Daniele, L. Macera, C. Mondelli, *J. Am. Ceram. Soc.* doi:10.1111/jace.15112.
- [89] S. Bastone, D. F. C. Martino, V. Renda, M. L. Saladino, G. Poggi, E. Caponetti. *Colloids Surf. A: Physicochem. Eng. Aspects* **513**, 241 (2017).
- [90] K. Kudłacz. *Phase Transitions within the Lime Cycle: Implications in Heritage Conservation*. PhD Thesis, University of Granada, Granada (2013).
- [91] Y. Ding, G. Zhang, H. Wu, B. Hai, L. Wang, Y. Qian. *Chem. Mater.* **13**, 435 (2001).
- [92] R. Giorgi, C. Bozzi, L. Dei, C. Gabbiani, B. W. Ninham, P. Baglioni. *Langmuir* **21**, 8495 (2005).
- [93] E. Ciliberto, G. G. Condorelli, S. La Delfa, E. Viscuso. *Appl. Phys. A*, **92**, 137 (2008).
- [94] P. D'Armada, E. Hirst. *J. Architect. Conserv.* **18**, 63 (2012).
- [95] C. Rodríguez-Navarro, K. Elert, R. Ševčík. *CrystEngComm* **18**, 6594 (2016).
- [96] A. Otero, E. Charola, C. A. Grissom, V. Starinieri. *Ge-conservación* **1**, 71 (2017).
- [97] V. Nikulshina, M. E. Galvez, A. Steinfeld. *Chem. Eng. J.* **129**, 75 (2007).
- [98] S. M. Shih, C. S. Ho, Y. S. Song, J. P. Lin. *Ind. Eng. Chem. Res.* **38**, 1316 (1999).
- [99] G. Montes-Hernandez, A. Pommerol, F. Renard, P. Beck, E. Quirico, O. Brissaud. *Chem. Eng. J.* **161**, 250 (2010).
- [100] D. T. Beruto, R. Botter. *J. Eur. Ceram. Soc.* **20**, 497 (2000).
- [101] Ö. Cizer, C. Rodríguez-Navarro, E. Ruiz-Agudo, J. Elsen, D. Van Gemert, K. van Balen. *J. Mater. Sci.* **47**, 6151 (2012).
- [102] G. M. Bond, J. Stringer, D. K. Brandvold, F. A. Simsek, M. G. Medina, G. Egeland. *Energy Fuels*, **15**, 309 (2001).
- [103] K. Van Balen. *Cem. Concr. Res.* **35**, 647 (2005).
- [104] P. López-Arce, L. S. Gómez-Villalba, S. Martínez-Ramírez, M. Álvarez de Buergo, R. Fort. *Powder Technol.* **205**, 263 (2011).

- [105] T. Yang, B. Keller, E. Gagyari, K. Hametner, D. Günther. *J. Mater. Sci.* **38**, 1909 (2003).
- [106] R. M. Dheilly, J. Tundo, Y. Sebaïbi, M. Quéneudec. *Construction Building Mater.* **16**, 155 (2002).
- [107] E. Ruiz-Agudo, K. Kudłacz, C. V. Putnis, A. Putnis, C. Rodríguez-Navarro. *Environm. Sci. Technol.* **47**, 11342 (2013).
- [108] P. López-Arce, L. S. Gómez-Villalba, L. Pinho, M. E. Fernández-Valle, M. Álvarez de Buergo, R. Fort. *Mater. Characterization* **61**, 168 (2010).
- [109] L. S. Gomez-Villalba, P. López-Arce, M. Alvarez de Buergo, R. Fort. *Appl. Phys. A* **104**, 1249 (2011).
- [110] L. S. Gomez-Villalba, P. López-Arce, R. Fort. *Appl. Phys. A* **106**, 213 (2012).
- [111] V. Daniele, G. Taglieri. *J. Cult. Herit.* **11**, 102 (2010).
- [112] P. López-Arce, A. Zornoza-Indart. *Appl. Phys. A* **120**, 1475 (2015).
- [113] C. Rodríguez-Navarro, I. Vettori, E. Ruiz-Agudo. *Langmuir*, **32**, 5183 (2016).
- [114] H. Nielsen, S. Aloni, J. J. De Yoreo. *Science* **345**, 1158 (2014).
- [115] C. Rodríguez-Navarro, K. Kudłacz, Ö. Cizer, E. Ruiz-Agudo. *CrystEngComm* **17**, 58 (2015).
- [116] K. Sand, J. D. Rodríguez-Blanco, E. Makovicky, L. G. Benning, S. L. S. Stipp. *Cryst. Growth Des.* **12**, 842 (2012).
- [117] E. Carretti, D. Chelazzi, G. Rocchigiani, P. Baglioni, G. Poggi, L. Dei. *Langmuir* **29**, 9881 (2013).
- [118] G. Ziegenbalg. in *Cultural Heritage Preservation, Proceedings of the European Workshop*, M. Krüger (Ed.), pp. 240–245, Fraunhofer IRB Verlag, Stuttgart (2011).
- [119] A. Arizzi, L. S. Gómez-Villalba, P. López-Arce, G. Cultrone, R. Fort. *Eur. J. Miner.* **27**, 311 (2015).
- [120] Z. Slizkova, D. Frankeová. in *Proc. 12th Int. Congress on the Deterioration and Conservation of Stone*, G. Wheeler (Ed.), pp. 1–10, Columbia University, New York (2012).
- [121] S. Sequeira, C. Casanova, E. J. Cabrita. *J. Cult. Herit.* **7**, 264 (2006).
- [122] G. Borsoi, B. Lubelli, R. van Hees, R. Veiga, A. S. Silva. *Construct. Building Mater.* **142**, 385 (2017).
- [123] P. Baglioni, E. Carretti, D. Chelazzi. *Nat. Nanotech.* **10**, 287 (2015).
- [124] P. Baglioni, R. Carrasco Vargas, D. Chelazzi, M. Colón González, A. Desprat, R. Giorgi. *Studies Conservation* **51**, 162 (2006).
- [125] L. S. Gómez-Villalba, P. López-Arce, A. Zornoza, M. Álvarez de Buergo, R. Fort. *Boletín Soc. Española Ceram. Vidrio* **50**, 85 (2011).
- [126] M. Lichelli, M. Malagodi, M. Weththimuni, C. Zanchi. *Appl. Phys. A* **114**, 673 (2014).
- [127] E. Maryniak-Piaszczyński, P. Egloffstein, G. Ziegenbalg. in *Proc. 11th Int. Congr. Deterioration and Conservation of Stone*, J. W. Lukaszewicz, P. Niemcewicz (Eds.), pp. 1247–1256, Nicolaus Copernicus University, Torun, Poland (2008).
- [128] G. Borsoi, M. Tavares, R. Veiga, A. S. Silva. *Microscopy Microanal.* **18**, 1181 (2012).
- [129] G. Borsoi, M. Tavares, R. Veiga, A. S. Silva. *Mater. Sci. Forum* **730**, 942 (2013).
- [130] A. M. Barberena-Fernández, M. San Andrés-Moya, P. M. Carmona-Quiroga, M. T. Blanco-Varela. in *Science, Technology and Cultural Heritage*, M. A. Rogerio-Canderera (Ed.), pp. 127–132. Taylor-Francis, London (2014).
- [131] D. M. R. Costa, A. S. Leal, J. M. Mimoso, S. R. M. Pereira. in *Proc. Int. Conference Glazed Ceramics in Architectural Heritage*, pp. 269–278. Laboratório Nacional Engenharia Civil, Lisbon (2015).
- [132] M. Lanzón, J. A. Madrid, A. Martínez-Arredondo, S. Mónaco. *Appl. Surf. Sci.* **424**, 20 (2017).
- [133] J. Gillon. *Nature* **415**, 847 (2002).
- [134] D. Chelazzi, R. Giorgi, P. Baglioni. *Macromol. Symposia* **238**, 30 (2006).
- [135] F. Andriulo, R. Giorgi, C. Steindal, P. Baglioni. *Pure Appl. Chem.* **89**, 29 (2017).
- [136] A. Campbell, A. Hamilton, T. Stratford, S. Modestou, I. Ioannou. in *Proc. Symp. 2011–Adhesives and Consolidants for Conservation: Research and Application*, pp. 17–21. Canadian Conservation Institute, Ottawa (2011).
- [137] C. Miliani, M. L. Velo-Simpson, G. W. Scherer. *J. Cult. Herit.* **8**, 1 (2007).
- [138] G. Borsoi, B. Lubelli, R. van Hees, R. Veiga, A. S. Silva. *J. Cult. Herit.* **18**, 242 (2016).
- [139] S. Gali, C. Ayora, P. Alfonso, E. Tauler, M. Labrador. *Cem. Concr. Res.* **31**, 933 (2001).
- [140] F. Lippmann. *Sedimentary Carbonate Minerals*, Springer-Verlag, Berlin (1973).
- [141] E. Tedesco, I. Mičetić, S. G. Ciappellano, C. Micheletti, M. Venturini, F. Benetti. *Toxicol. Vitro*, **29**, 1736 (2015).